



EDGEWOOD

CHEMICAL BIOLOGICAL CENTER

U.S. ARMY RESEARCH, DEVELOPMENT AND ENGINEERING COMMAND

ECBC-TR-639

DEVELOPMENT OF A VERSATILE CONDITIONING WIND TUNNEL FOR EVAPORATIVE FATE STUDIES

Daniel J. Weber
Daniel Waysbort
Clayton S. Moury
H. Dupont Durst

RESEARCH AND TECHNOLOGY DIRECTORATE

James E. Danberg



SCIENCE APPLICATIONS
INTERNATIONAL CORPORATION
Gunpowder, MD 21010-0068

October 2009

Approved for public release;
distribution is unlimited.



ABERDEEN PROVING GROUND, MD 21010-5424

Disclaimer

The findings in this report are not to be construed as an official Department of the Army position unless so designated by other authorizing documents.

REPORT DOCUMENTATION PAGE				Form Approved OMB No. 0704-0188	
Public reporting burden for this collection of information is estimated to average 1 hour per response, including the time for reviewing instructions, searching existing data sources, gathering and maintaining the data needed, and completing and reviewing this collection of information. Send comments regarding this burden estimate or any other aspect of this collection of information, including suggestions for reducing this burden to Department of Defense, Washington Headquarters Services, Directorate for Information Operations and Reports (0704-0188), 1215 Jefferson Davis Highway, Suite 1204, Arlington, VA 22202-4302. Respondents should be aware that notwithstanding any other provision of law, no person shall be subject to any penalty for failing to comply with a collection of information if it does not display a currently valid OMB control number. PLEASE DO NOT RETURN YOUR FORM TO THE ABOVE ADDRESS.					
1. REPORT DATE (DD-MM-YYYY) XX-10-2009		2. REPORT TYPE Final		3. DATES COVERED (From - To) Aug 05 - May 07	
4. TITLE AND SUBTITLE Development of a Versatile Conditioning Wind Tunnel for Evaporative Fate Studies				5a. CONTRACT NUMBER	
				5b. GRANT NUMBER	
				5c. PROGRAM ELEMENT NUMBER 6R27CZ	
6. AUTHOR(S) Weber, Daniel J.; Waysbort*, Daniel; Moury, Clayton S.; Durst, H. Dupont (ECBC); and Danberg, James E. (SAIC)				5d. PROJECT NUMBER	
				5e. TASK NUMBER	
				5f. WORK UNIT NUMBER	
7. PERFORMING ORGANIZATION NAME(S) AND ADDRESS(ES) DIR, ECBC, ATTN: RDCB-DRT-S, APG, MD 21010-5424 SAIC, P.O. Box 68, Gunpowder, MD 21010-0068				8. PERFORMING ORGANIZATION REPORT NUMBER ECBC-TR-639	
9. SPONSORING / MONITORING AGENCY NAME(S) AND ADDRESS(ES) DTRA, 8725 John J. Kingman Road, MS 6201, Fort Belvoir, VA 22060-6201				10. SPONSOR/MONITOR'S ACRONYM(S)	
				11. SPONSOR/MONITOR'S REPORT NUMBER(S)	
12. DISTRIBUTION / AVAILABILITY STATEMENT Approved for public release; distribution is unlimited.					
13. SUPPLEMENTARY NOTES * On leave from the Israel Institute for Biological Research, Ness Ziona, Israel					
14. ABSTRACT This report documents the development of a conditioning wind tunnel that allows multiple test samples to be conditioned at identical environmental settings that are used in smaller vapor sampling wind tunnels. The conditioning of multiple samples, especially those involving persistent chemicals, allows for the efficient use of a limited number of instrumented vapor sampling tunnels. Up to nine samples can be sequentially and quickly cycled through the instrumented vapor wind tunnels for a relatively short period of time to take vapor samples. The development of the conditioning wind tunnel progress through several iterations, starting as a smaller test cell and ultimately ending as a more conventional wind tunnel design. The tunnel was fabricated and the boundary-layer profile in the test section was measured at several locations. Analysis of the boundary-layer indicated that the profiles were in good agreement with the stipulated operational wind profiles. Recommendations for possible future improvements are also provided. The conditioning wind tunnel's versatility allows multiple droplet experiments with minor modifications enabling determination of volatilization of tens of milligrams of chemicals from 20 x 10 cm surfaces.					
15. SUBJECT TERMS					
Chemical	Boundary-layer	Law of the Wall	Law of the Wake		
Evaporation	Laminar	Coles' Law	Droplet		
Agent fate	Turbulent	Hot wire anemometry			
16. SECURITY CLASSIFICATION OF:			17. LIMITATION OF ABSTRACT	18. NUMBER OF PAGES	19a. NAME OF RESPONSIBLE PERSON Sandra Johnson
a. REPORT U	b. ABSTRACT U	c. THIS PAGE U	UL	61	19b. TELEPHONE NUMBER (include area code) (410) 436-2914

Blank

PREFACE

The work described in this report was authorized under Program Element No. 6R27CZ for the Defense Threat Reduction Agency. This work was started in August 2005 and completed in May 2007.

The use of either trade or manufacturers' names in this report does not constitute an official endorsement of any commercial products. This report may not be cited for purposes of advertisement.

This report has been approved for public release. Registered users should request additional copies from the Defense Technical Information Center; unregistered users should direct such requests to the National Technical Information Service.

Acknowledgments

The authors acknowledge Dr. Carol Brevett (SAIC), who proposed the original idea for a Conditioning Wind Tunnel; John Molnar (SAIC) for assisting with the development and assembly of the conditioning wind tunnel; Miles Miller (SAIC) for his comments on the design and assistance with editing the final report; John Pence, Wendel Shuely, Drs. Bruce King, and Robert Nickol (SAIC) for their comments and suggestions with regard to the design of the wind tunnel; Daniel Ward, Glen Wetherell, James Rogers, Courtney Johnson, Daniel Lumpkins, Ryan O'Malley, Matthew Goodwin, Richard Moore, and James Orndoff (U.S. Army Edgewood Chemical Biological Center) for their contributions in fabricating the numerous parts of the conditioning tunnel.

Blank

CONTENTS

1.	INTRODUCTION	9
2.	EVAPORATION TEST CELL	10
2.1	Evaporation Test Cell Design	11
2.2	Evaporation Test Cell Characterization	12
3.	CONDITIONING WIND TUNNEL	19
3.1	Design	19
3.1.1	Plenum Box	20
3.1.2	Flow Straighteners	20
3.1.3	Settling Chamber and Contraction Section	22
3.1.4	Fetch Section and Roughening Elements	23
3.1.5	Test Section	25
3.1.6	Exit Section	28
3.1.7	Turning Vane Section	28
3.1.8	Sealing	29
3.1.9	Environmental Conditioning and Instrumentation	29
3.2	Conditioning Tunnel Flow Field Characterization	30
4.	VELOCITY PROFILE ANALYSIS	33
4.1	Regions of a Fully Developed, Equilibrium Turbulent Boundary Layer	33
4.2	Logarithmic-Region	34
4.3	Operational Profile	34
5.	MEASURE VELOCITIES COMPARED TO “OPERATIONAL” PROFILE	35
6.	“LAW OF THE WAKE” ANALYSIS	38
6.1	Coles’ Wake Function	39
6.2	Comparison of Channel Flow Operation Profile with Wake and Experimental Data	39
6.3	Channel Flow	41
6.4	Optimum Coles’ Wake Function Parameters for Experimental Profiles	41
6.5	Discussion of Table 2 Results	42

7.	SUGGESTED METHODS OF OPERATION	46
8.	CONCLUSIONS	47
9.	RECOMMENDATIONS.....	47
	LITERATURE CITED.....	49
	APPENDIX: CONDITIONING TUNNEL DESIGN DRAWING	51

FIGURES

1.	Prototype Evaporation Cell	11
2.	5 cm Inlet and Exhaust Ports for Evaporation Cell.....	12
3.	Schematic of Evaporation 1 cm Test Cell Velocity Profile Locations	13
4.	1 cm Evaporation Test Cell Configuration Characterization Profiles.....	14
5.	Schematic of Evaporation 5 cm Test Cell Velocity Profile Locations	15
6.	5 cm Evaporation Test Cell Configuration Characterization Profiles.....	16
7.	Representation of Smoke Visualization in 5 cm Evaporation Test Cell....	17
8.	Evaporation Test Cell with Straight/Divided Inlet and Exhaust Ports	18
9.	Close Up of Straight/Divided Inlet Ports.....	18
10.	1 cm Evaporation Test Cell with Straight/Divided Ports Velocity Profiles.....	19
11.	5 x 10 cm Conditioning Wind Tunnel	20
12.	Cross Section Schematic of 5 x 10 cm Conditioning Wind Tunnel	21
13.	Flow Straightener.....	22
14.	Design Spreadsheet Top Contour View of Conditioning Wind Tunnel.....	23
15.	Settling Chamber and Contraction Section	24
16.	Fetch Section with Roughening Elements	25
17.	Test Section Floor Installed and in Lowered Position	27
18.	Fetch, Test, and Exit Section Components.....	28
19.	Turning Vane Section	29
20.	Velocity Profile Characterization Test Setup.....	30
21.	Velocity Profile Characterization, Medium Velocity Case.....	32

22.	Velocity Profile Characterization, High Velocity Case	32
23.	Regions of the Turbulent Boundary-Layer	33
24.	Medium Velocity Profile, Velocity vs. Log(y)	35
25.	High Velocity Profile, Velocity vs. Log(y).....	36
26.	Least Squares Curve Fit of Medium Velocity Profiles (5 points)	37
27.	Least Squares Curve Fit of High Velocity Profiles (5 points).....	37
28.	Comparison of Operation Profile with and without Wake to Conditioning Tunnel Data, Medium Wind Velocity	40
29.	Comparison of Operation Profile with and without Wake to Conditioning Tunnel Data, High Wind Velocity	40
30.	Comparison Between Predicted Law of the Wake and Centerline Velocity Measurements for High and Medium Speed Conditions	44
31.	Comparison Between Predicted Law of the Wake Based on Average Parameters and Medium Wind Speed Data.....	45
32.	Comparison Between Predicted Law of the Wake Based on Average Parameters and High Wind Speed Data	45

TABLES

1.	Conditioning Tunnel Linear Regression Analysis Results.....	38
2.	Conditioning Tunnel Velocity Profile Parameters.....	43

DEVELOPMENT OF A VERSATILE CONDITIONING WIND TUNNEL FOR EVAPORATIVE FATE STUDIES

1. INTRODUCTION

The use of chemical warfare agents (CWA) is a possible threat by terrorists or military organizations against military targets and civilian populations. The release of toxic industrial chemicals (TICs) and toxic industrial materials (TIMs), either accidentally or on purpose, also poses a threat to civilian populations. A decrease of the number of casualties, as well as collateral damage, can be achieved by an understanding of the evaporation, transport, and diffusion that the agent is expected to follow. Also, knowledge of the time dependent release of the agent vapor from the contamination origin is required. This information can be used in computer models for predicting the development of hazardous situations.

A major obstacle in developing accurate models is the characterization of the interaction between the agent and the surface in the volatilization of the CWA under operational environmental conditions. This is complicated by the large number of variables associated with this evaporation process. The current approach to overcome this problem is to measure the evaporation rates of various threat agents from representative surface materials. Field testing is one way to measure this interaction because the measurements are done while the process is occurring in a real environment under typical meteorological conditions. Yet, the high mammalian toxicity of the CWA requires extraordinary safety precautions that tend to increase the complexity and decrease the practicality of conducting experiments in the open environment. Also, the results of field experiments suffer from inaccuracies in the measurements due to the inability to control the outdoor environmental conditions: temperature, wind speed and direction, solar loading, humidity, atmospheric pressure, and other parameters that vary constantly throughout the day and night. Thus, laboratory experiments provide an alternative approach, where a properly designed experimental apparatus provides adequate control over the desired atmospheric test conditions under laboratory conditions, allowing their effects on the evaporation process of CWAs to be studied. Chemical warfare agent type, drop size, material surface type, temperature, wind speed, and relative humidity are the main variables of interest and can be simulated in a laboratory. Accordingly, laboratory experiments may serve as a good substitution for field testing.

In the case of wind speed, the portion of the atmospheric velocity profile near the drop has a direct effect on evaporation. Operationally, wind speed data are usually acquired at heights up to 2 m above the ground by meteorological stations. Typical agent drop heights are on the order of a millimeter. Thus, for accurate experimental results, it is important that the velocity only in the vicinity of the drop be replicated in the experimental test facility. Due to the small size of the test cells and wind tunnels, special care is required in their aerodynamic design to develop boundary layer profiles that match the part of the atmospheric boundary layer near the ground.

The 5 cm Agent Fate Wind Tunnel (test section cross-section = 5 x 5 cm) was built to measure the volatilization of a minimum of a single drop of CWA from various surfaces in support of the Agent Fate program.^{1,2} Drop sizes ranging from 1 to 9 μL were tested. The tunnel was designed to fit inside a standard chemical fume hood, supply properly conditioned air (temperature and humidity) with the appropriate velocity profile near the drop, and thoroughly mix the resulting agent vapor for sampling at the tunnel exhaust. Typically, only a few hours were required to test a non-persistent CWA. Accordingly, one or two tests could be completed in a day depending on the agent and the test conditions. However, for a persistent CWA, up to several days or even weeks were required to conduct a single drop evaporation test. Due to the number of persistent CWAs and test conditions desired for testing, insufficient time was available for completion of the test program. A Conditioning Wind Tunnel or Test Cell is a potential solution to this problem.

The Conditioning Wind Tunnel provides the same environmental conditions (temperature, humidity, and wind speed) as were present in the 5 cm Agent Fate Wind Tunnels, but allows as many as eight test specimens (agent/substrate) to be tested concurrently. Unlike the 5 cm Agent Fate Wind Tunnel, which includes sophisticated vapor measuring instrumentation, the Conditioning Wind Tunnel merely maintains a constant environment. After a period of testing (and volatilization measurement) in the 5 cm Agent Fate Wind Tunnel, the drop/substrate would be moved to the Conditioning Wind Tunnel for continued exposure (conditioning) at the same test conditions. The drop/substrate would then be periodically returned to the 5 cm Wind Tunnel for measurements. Thus, nine samples (eight in the Conditioning Wind Tunnel and one in the 5 cm Agent Fate Wind Tunnel) could be tested simultaneously. This would greatly increase the throughput of the experimental procedure and make more efficient use of the capabilities of the 5 cm Agent Fate Wind Tunnel.

In addition, a wind tunnel that contains multiple drops is more desirable. Testing multiple drops provides a better approximation of the disseminated drops from an actual CW attack, thus allowing the associated interactions between drops that effect evaporation to be measured.

This report describes a Conditioning Wind Tunnel that was designed and built for keeping eight 5 cm Wind Tunnel samples in identical environmental conditions (including the velocity profile) as in the 5 cm Agent Fate Wind Tunnel. In addition, with minor changes to the test section floor insert, the volatilization of multiple drops of CWAs and TICs from a 20 x 10 cm substrate surface of a selected material can be obtained.

2. EVAPORATION TEST CELL

The design and development of the Conditioning Wind Tunnel progressed through an evolutionary process. When the idea first arose for a new agent fate wind tunnel, the initial design focus was to provide the ability to test multiple drops.

The 5 cm Agent Fate Wind Tunnel could test single or multiple drops but was limited to only a few small drops due to its small test section (a constraint imposed to allow it to fit within a standard chemical fume hood). A wind tunnel large enough to test multiple drops was more desirable in that multiple drops approached a real world scenario and allows investigation of interactions existing among the disseminated drops on the surface. More drops yield more vapor mass, which increased measurability. Thus, the influence of the droplet to droplet interaction could be measured and compared to the single drop measurements made in the 5 cm Agent Fate Wind Tunnels.

2.1 Evaporation Test Cell Design.

Initial investigations for a Conditioning Wind Tunnel were performed on a configuration based on an Evaporation Test Cell used in a prior study at the Israel Institute for Biological Research (Ness Ziona, Israel). The dimensions of the Evaporation Test Cell were: 20 cm x 10 cm with an adjustable height of 1 to 5 cm, which permitted multiple drops to be tested simultaneously.³ Changing the height of the test cell was done by replacing the sample carrier and the inlet/outlet ports. The test cell is shown in Figure 1. The air enters through the inlet port on the left, proceeds through a vertical 90° expansion, flows across the evaporation cell and exhausts to the right through a horizontal 90° contraction port on the left. Different cell heights could be achieved by exchanging the aluminum floor with a different thickness block, and replacing the inlet and exhaust ports with matching height dimensions. The cell is shown in the 1 cm high configuration. The 5 cm cell height inlet and exhaust ports are shown in Figure 2.

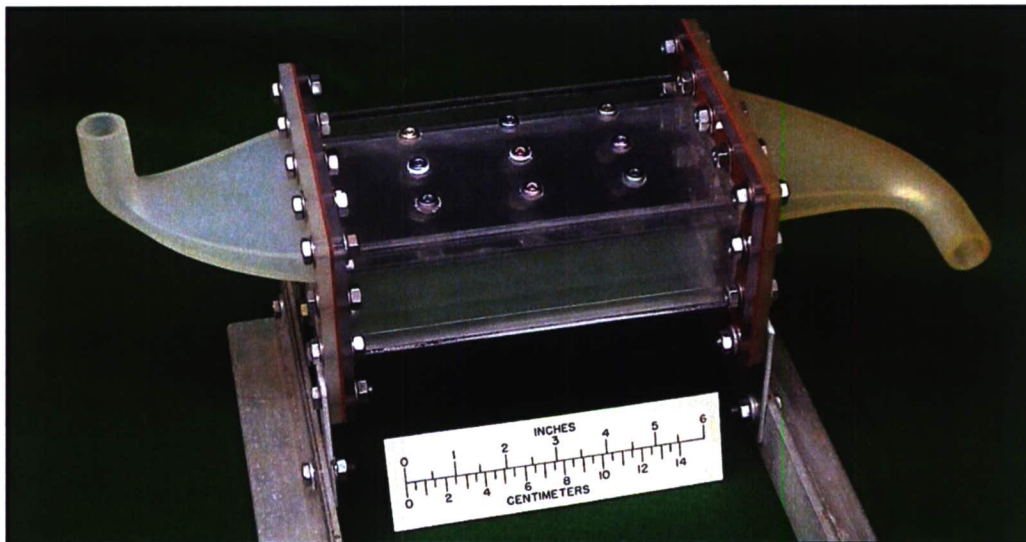


Figure 1. Prototype Evaporation Cell

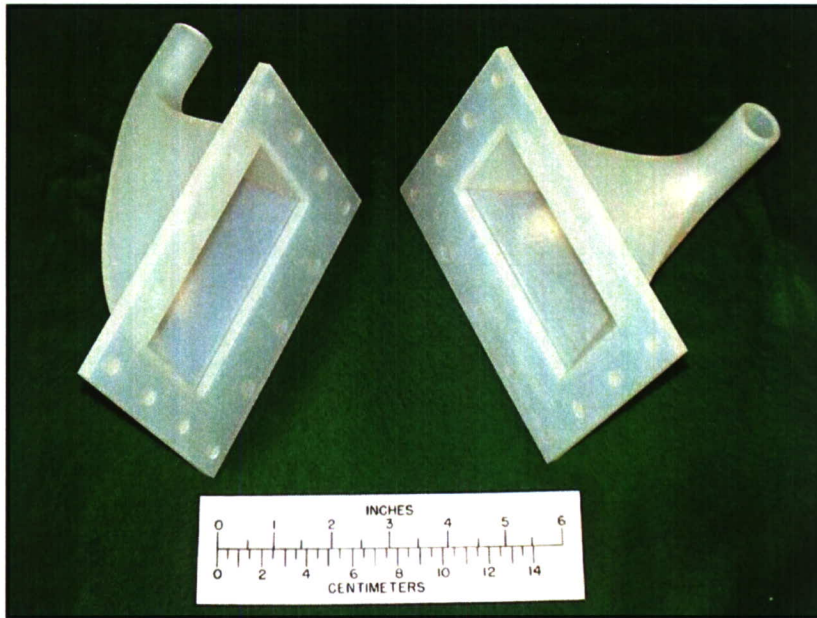


Figure 2. 5 cm Inlet and Exhaust Ports for Evaporation Cell

2.2 Evaporation Test Cell Characterization.

The nine 1/8 in. pipe plugs in the ceiling of the test cell were used for characterization of the airflow field through the cell. The characterization process was a variation on the methodology developed for the 5 cm Agent Fate Wind Tunnels.⁴ Wind speeds of 0.5, 3.0, and 5.0 m/s at a height of 2 m were selected as test conditions by the Agent Fate Program.⁵ Using smooth wall, turbulent boundary-layer theory, these wind speeds were extrapolated to the ground, thereby establishing the Agent Fate Program's three operational velocity profiles. For characterizing the Evaporation Test Cell, as well as the follow-on Conditioning Wind Tunnel, only the middle and high velocity profiles were used. The low speed profile tended to be problematic in the areas of generation, measurements, and analysis, due to the low airflow rate and the influence of laminar effects.

It should be noted that during the data analysis after the experimental testing had been completed, an error was discovered in the how the operational profiles were originally developed for the Agent Fate program.[†] The wake term for the core region of the boundary layer was subtracted instead of added. This error has been corrected in the operational profiles depicted in the plots presented in this report. However, because the error was found after the completion of the experiments, the set velocity was typically lower than the operational velocity required. The operational velocity difference was more pronounced for the 1 cm high test cell than for the 5 cm cell due to the shorten height. Although the operational velocity was typically set low for the 1 cm test cell, the range of profiles from the various measurement positions still encompassed the correct operational profile.

[†] Excel spreadsheet provided by modelers containing operational profiles.

A series of velocity profiles were measured at positions A through G as shown in Figure 3. The test cell was set up for the 1 cm high configuration. A vacuum pump was attached to the horizontal exhaust and used to establish the required flow rate through the test cell that would generate a velocity of 1.28 m/s at 3.76 mm at position E, matching the mid operational wind profile. The velocity for the corrected operational profile should have been 1.44 m/s. The flow rate was controlled by an Aalborg mass flow controller.

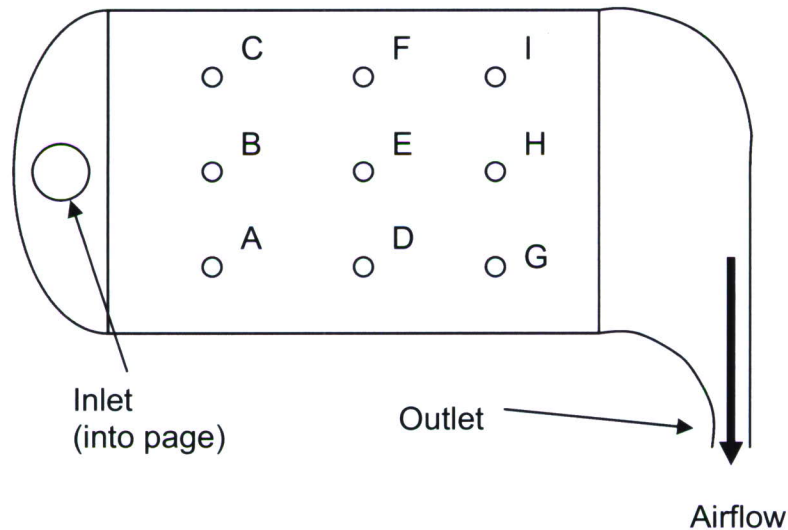


Figure 3. Schematic of Evaporation 1 cm Test Cell Velocity Profile Locations

The velocity profile characterization was performed using a single component hot wire anemometer system and positioning apparatus, which is described in detail in the 5 cm Agent Fate Wind Tunnel characterization report.⁴ The velocity profiles measured at the nine positions are shown in Figure 4.

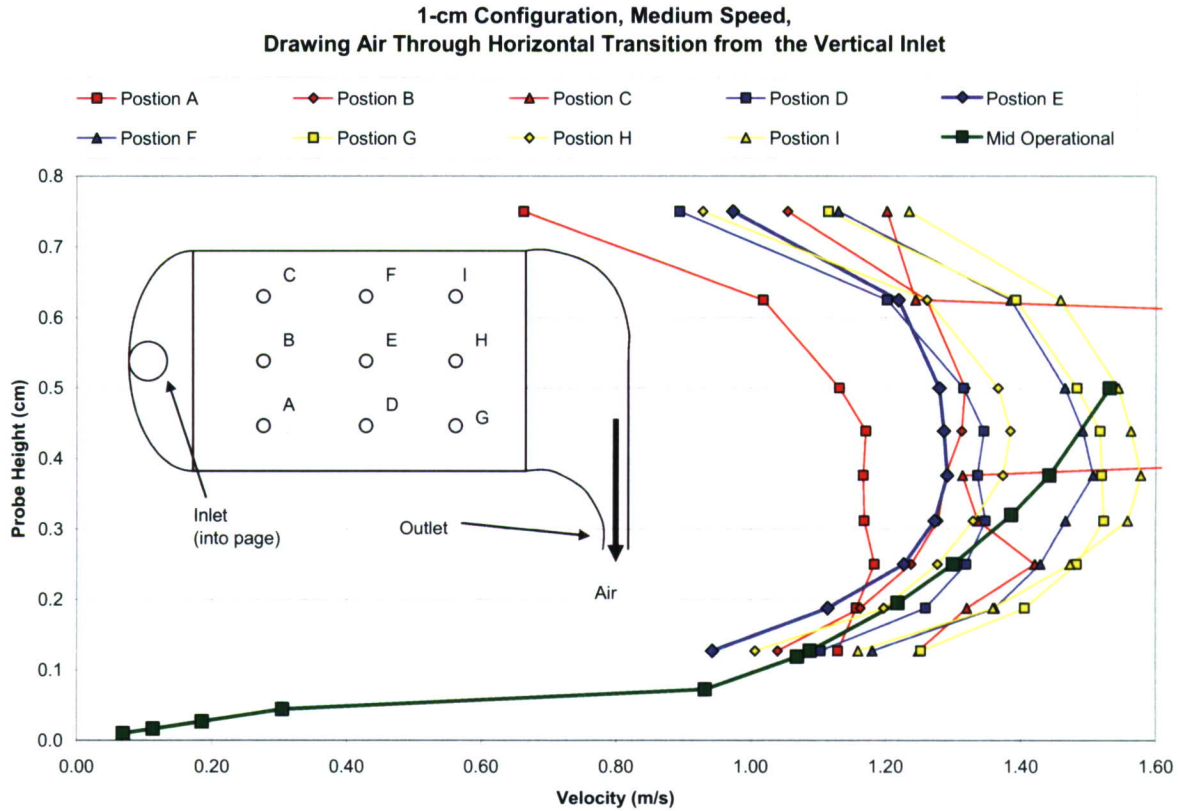


Figure 4. 1 cm Evaporation Test Cell Configuration Characterization Profiles

Only the centerline profiles (positions B, E, and H) showed respectable agreement with the medium speed operational profiles. Smoke visualization was used to determine the flow quality in the test cell. With all ports closed, the smoke indicated the desired absence of recirculation areas throughout the test cell and that the flow steadily moved from inlet to exhaust.

The Evaporation Test Cell configuration was tested next with the test section's 5 cm thick floor block replaced by a 1 cm thick block and switching out the 1 cm inlet and exhaust ports with 5 cm ports. Air was blown through the cell using a Miller-Nelson environmental conditioning unit and inlet mass flow controller as opposed to being pulled through by a vacuum as was previously done for the 1 cm configuration. The flow direction and probe positions are shown in Figure 5.

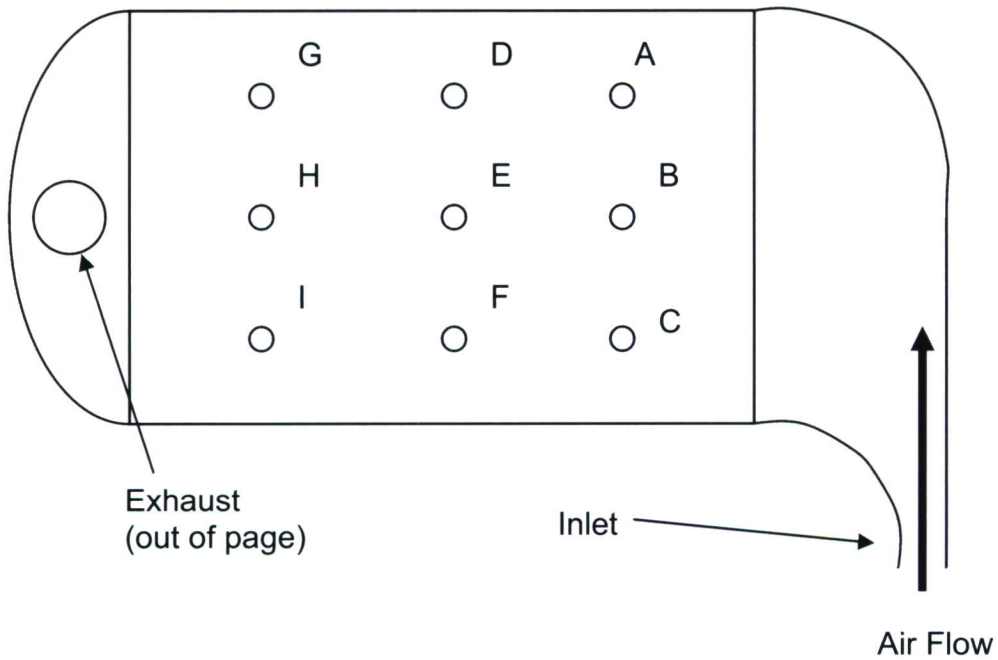


Figure 5. Schematic of Evaporation 5 cm Test Cell Velocity Profile Locations

The flow rate was established at position E at a height of 0.5 cm above the test section floor for a velocity of 1.42-m/s (corresponding to the mid Agent Fate uncorrected operational velocity profile of 3.0 m/s at 2m). The corrected value was 1.44-m/s, which highlights the lack of influence of the wake region on the velocities nearer the surface for this height tunnel. With the flow rate held constant, profiles were measured at all nine probe locations (A thru I). The resulting profiles are shown in Figure 6. Along with the measurements at the nine positions, the Agent Fate mid operational velocity profile and the corresponding 5 cm Agent Fate Wind Tunnel profile are also shown. Symbols and lines of the same color represents the three profiles at the same downstream location, but different cross stream positions, whereas the same plotting symbol (e.g., squares, diamonds, and triangles) represents the profiles at different down stream positions but at the same cross stream locations.

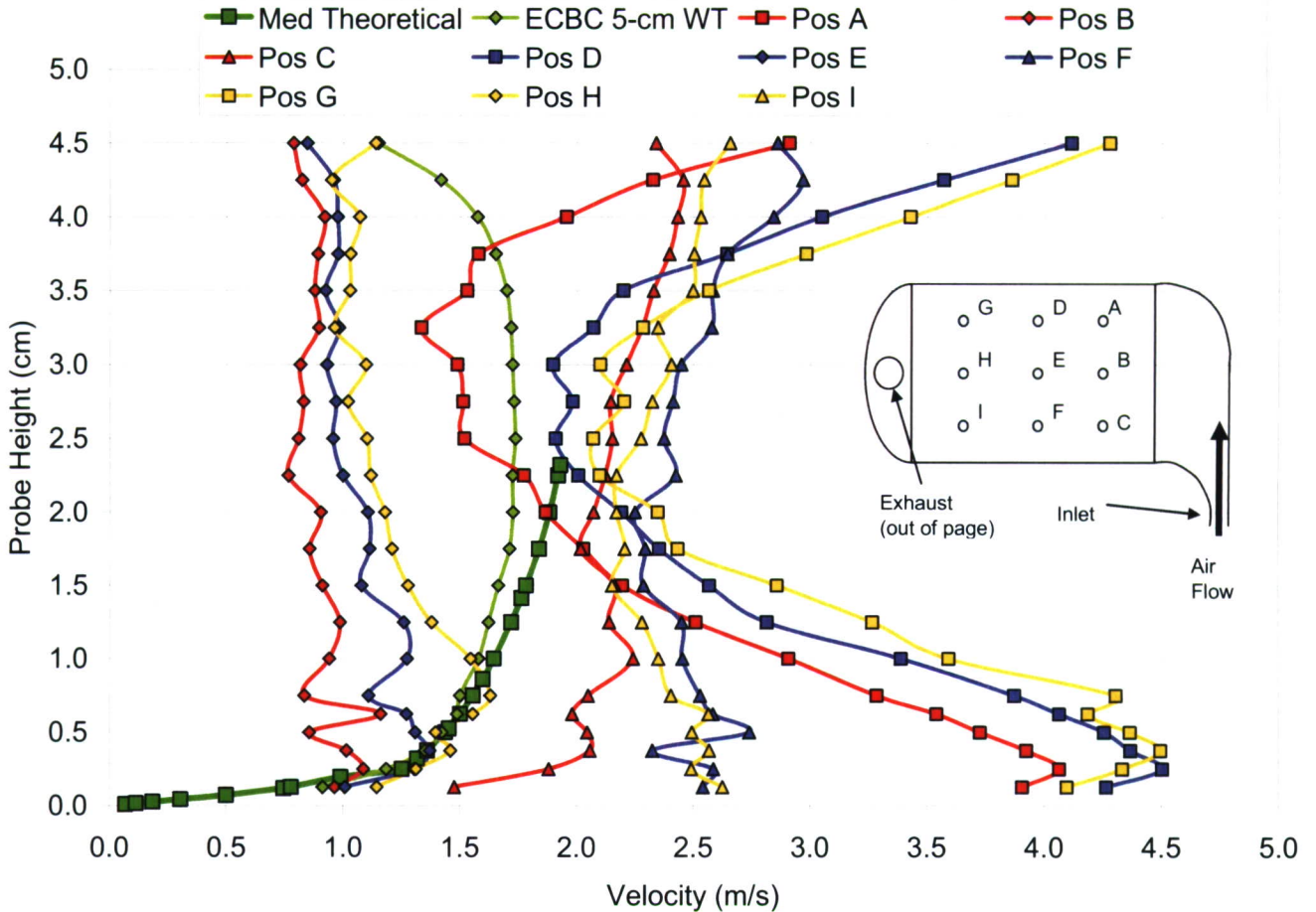


Figure 6. 5 cm Evaporation Test Cell Configuration Characterization Profiles

As can be seen, the velocity profiles are very erratic. Although limited agreement with the operational profiles along the centerline positions below 0.5 cm height was obtained, the far side profiles (A, D, and G) exhibit a boundary layer profile opposite as to what was expected. The velocity was lowest in the center of the tunnel and increased as the floor and ceiling were approached, respectively. The near side profiles (C, F, and I) showed only a slight increase from the center velocities as the floor and ceiling are approached.

The reason for the poor agreement of the velocity profiles was probably due to flow separation at the inlet and the presence of a large recirculation region covering the majority of the test cell section. The centerline profiles (positions B, E, and H) are near the low velocity area of the recirculation region and may even be in an area of reversed flow, as are the profiles at positions C, F, and I. Smoke visualization of the flow field confirmed the presence of a recirculation region in the test cell. A sketch of the observed recirculation region is shown in Figure 7.

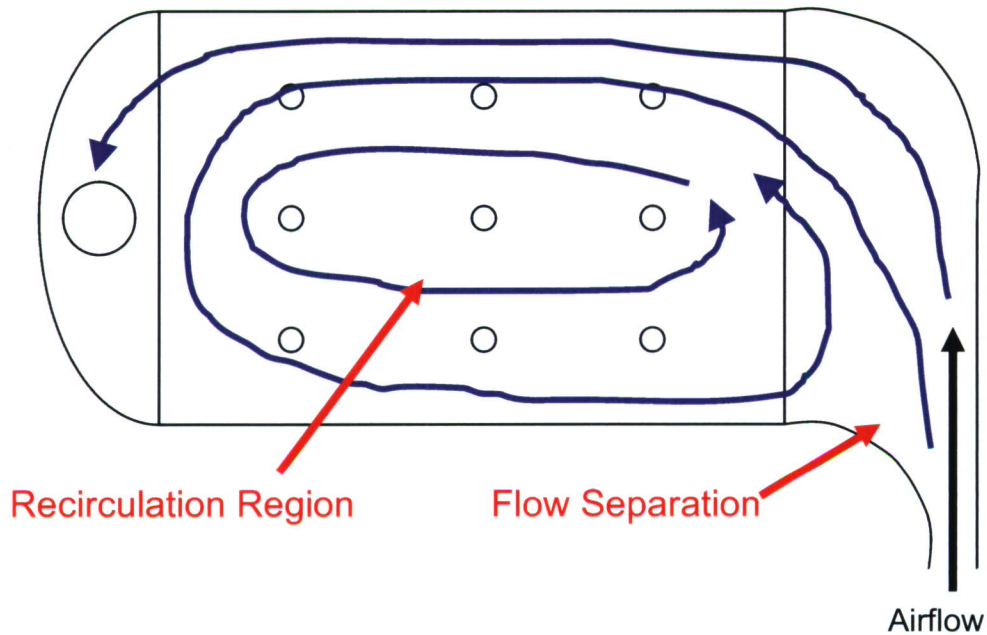


Figure 7. Representation of Smoke Visualization in 5 cm Evaporation Test Cell

New inlet and exhaust ports were fabricated for the 1 cm high test cell configuration. These ports were straight and divided internally into three equal volumes to facilitate splitting the flow evenly across the entrance to the test cell. Figure 8 shows the test cell with the new ports installed. Figure 9 is a close up of the inlet port highlighting the internal dividers. The mass flow controller was set to an appropriate flow rate to achieve the mid-operational velocity of 1.28 m/s at a height above the floor of 3.76 mm at position E.

The corresponding velocity profiles for the nine positions are presented in Figure 10. Agreement with the operational profile is fair for position A and the centerline positions, B, E, and H but is considerably poorer for the other positions.

Because of the requirement to match the operational velocity profiles, the Evaporation test cell was deemed to require further refinements. These might include a longer inlet section with a shallow angle expansion of the flow from the air supplying device, turning vanes, extend fetch section downstream of the turning vanes, and upstream of the test section to allow flow to establish and stabilize, and some type of roughening elements to trip the boundary-layer. Another modification might be to aerodynamically tailor the inlet port contour to try to improve the flow expansion from the air supply line to the test cell entrance. However, these approaches were not attempted because it was decided to pursue a more conventional tunnel design.

Due to the unsatisfactory results achieved with the Evaporation Test Cell, only limited testing was conducted. At this point in the program, a new chemistry

laboratory came online with 2.5 m wide chemical fume hoods. This allowed a larger Conditioning Wind Tunnel to be considered. At this time it was also decided to focus on a more conventional wind tunnel design that would enable up to eight, agent/substrate samples to be conditioned simultaneously. The 5 x 10 cm Conditioning Wind Tunnel (as it was now known) was designed to allow testing multiple drops or small pools on a variety of substrates as large as 10 cm x 20 cm long. This represented a more versatile facility that could either provide conditioning only or be instrumented with vapor sampling equipment for evaporation studies for a wide range of chemical studies.

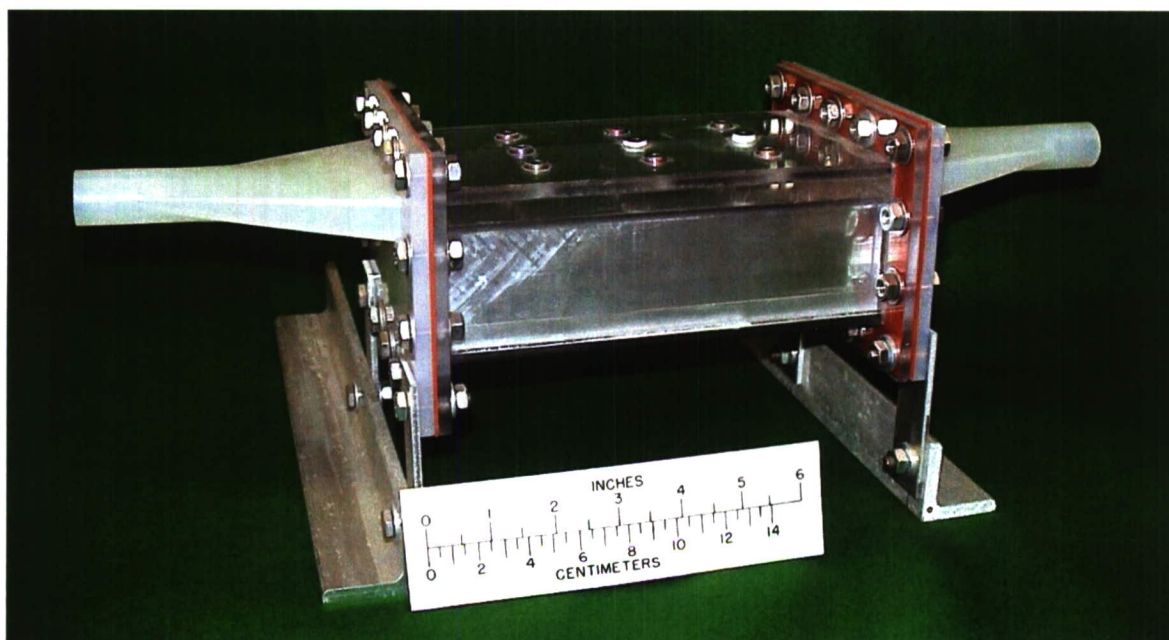


Figure 8. Evaporation Test Cell with Straight/Divided Inlet and Exhaust Ports

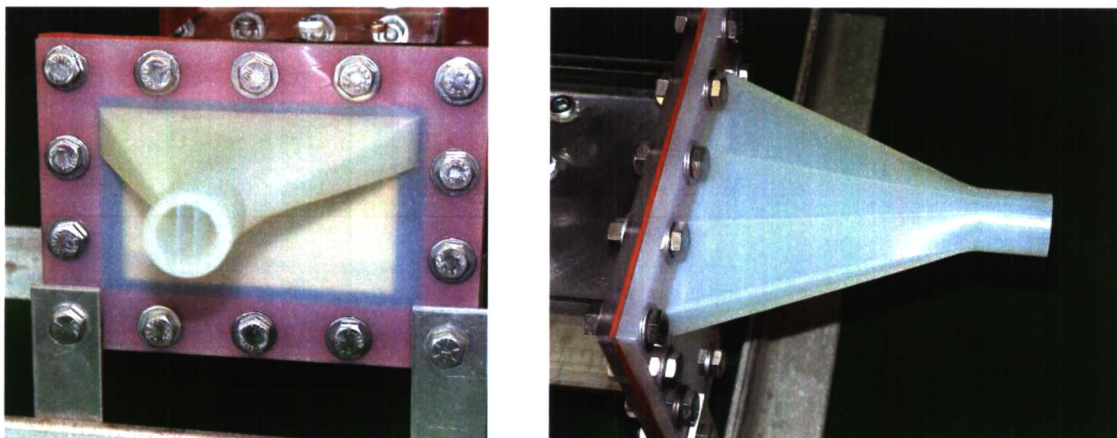


Figure 9. Close Up of Straight/Divided Inlet Ports

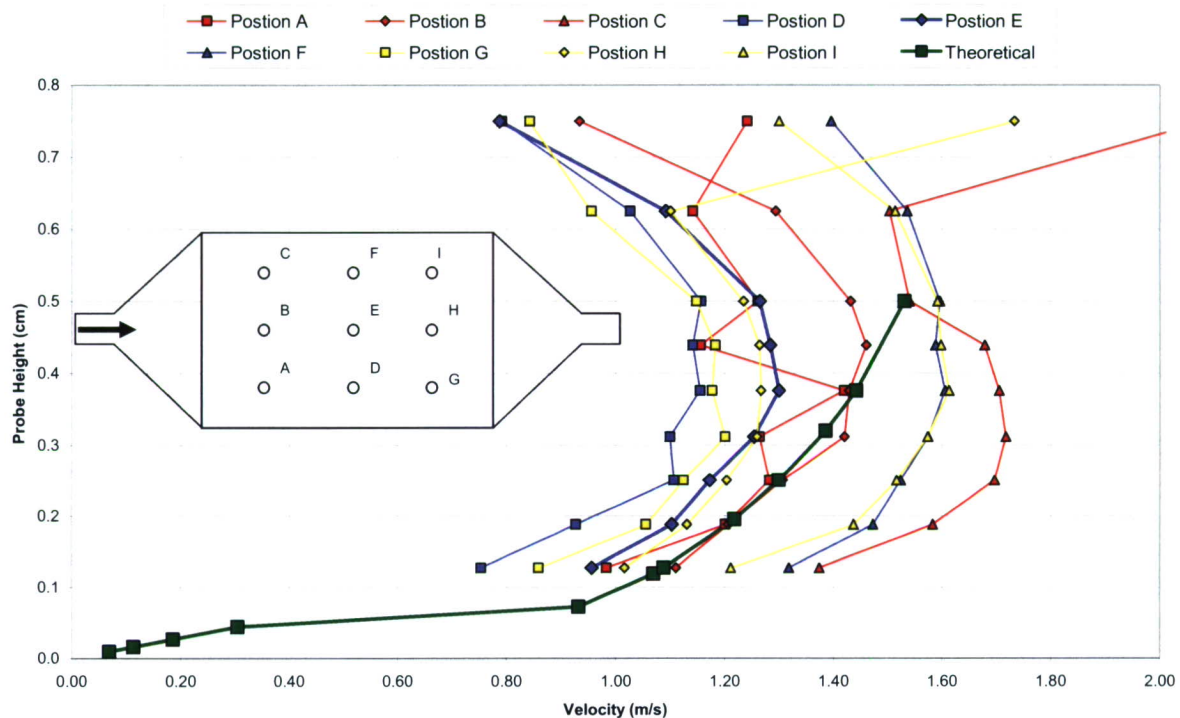


Figure 10. 1 cm Evaporation Test Cell with Straight/Divided Ports Velocity Profiles

3. CONDITIONING WIND TUNNEL

As a consequence of the results from the Evaporation Test Cell, a more conventional wind tunnel design was pursued. Initially, the design focused on variations of the 5 cm Agent Fate Wind Tunnel. Push and pull concepts were considered where the supply air would either be generated by a higher pressure at the inlet (push) or a vacuum at the exhaust (pull). A concern with relying on the 5 cm Agent Fate design was the use of its expanding inlet. The 5 cm Wind Tunnel inlet expanded the supply air line diameter of 1.3 cm to the 5 x 5 cm tunnel cross-section over a length of 33 cm, while maintaining a half angle of 3.5° to reduce flow separation. The 10 cm width of the Conditioning Wind Tunnel increased the length of the expanding inlet to 71 cm. This led to concerns that the flow might not expand uniformly and create problems in generating uniform flow in the test section.

3.1 Design.

The approach for the 5 x 10 cm Conditioning Wind Tunnel design was based on more traditional wind tunnel components, and also incorporated lessons learned from the 5 cm Agent Fate Wind Tunnel. The design process used the design criteria established by Barlow, et al⁶ and Bradshaw and Mehta⁷. Figure 11 shows a photograph of the Conditioning Wind Tunnel, and Figure 12 is a cross section schematic along the long axis of the wind tunnel. The major components of the tunnel

include a plenum box, flow straighteners, settling chamber and contraction section, fetch, roughening elements, test section, removable test section floor, exit section, and turning vane section. A complete set of design drawings for the 5 x 10 cm Conditioning Wind Tunnel can be found in the Appendix. Fabrication of the tunnel relied heavily on Stainless Steel (Type 304) in areas of possible agent contamination. The following sections describe each component in detail.

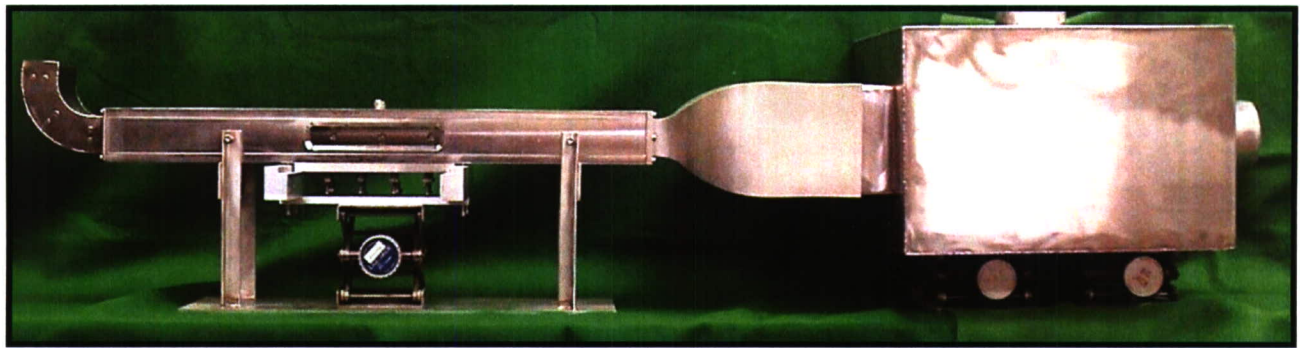


Figure 11. 5 x 10 cm Conditioning Wind Tunnel

3.1.1 Plenum Box.

The plenum box allows the pre-conditioned air to become thermally homogeneous and to eliminate any spurious air currents that might influence the air entering the tunnel inlet. The plenum box was constructed of thin gauge stainless steel sheet metal and was designed to accept conditioned air from a small diameter supply line. A baffle was installed just inside the box at the supply inlet, as seen in Figure 12. The baffle was to disperse the inlet flow to fill the plenum so that a more uniform flow would be presented to the flow straightening honey comb and screens at the contraction inlet. The plenum box measured 45.72 cm square by 30.23 cm high. A future modification would be to reduce the size of the plenum box thereby reducing the overall length of the wind tunnel.

3.1.2 Flow Straighteners.

The flow straightener assembly served two purposes. The first was to create sufficient flow restrictions to assist in generating a uniform flow. The second purposed was to introduce parallel laminar flow to the contraction section. The flow straighteners consisted of one section of aluminum honeycomb, 20 mm thick, with a cell size of 4.8 mm, and two 24 x 24 mm openings per inch with a wire diameter of 0.9 mm. The spacing between each screen and the screen and the honey comb is 20 mm. Figure 13 shows the honey comb screen assembly.

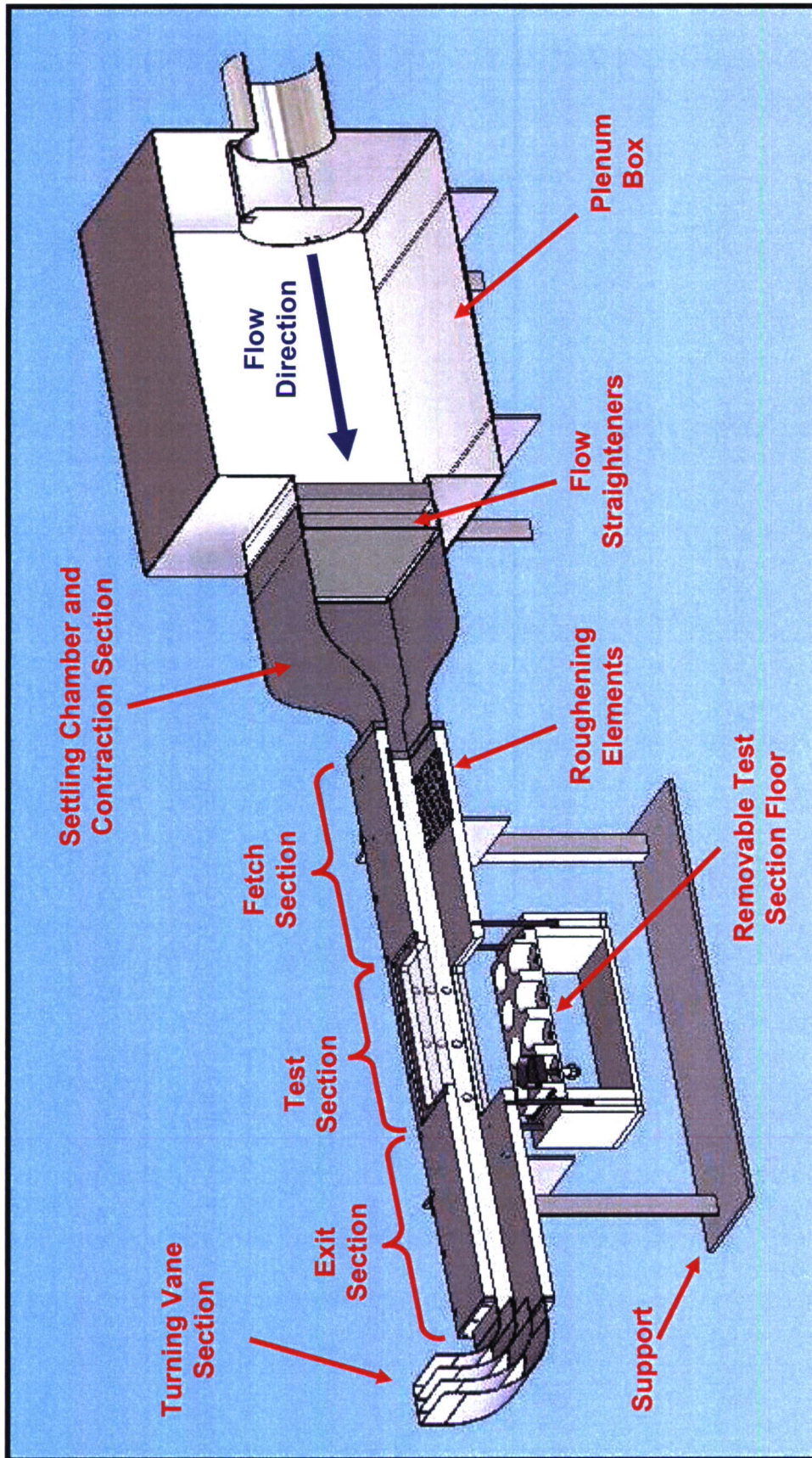


Figure 12. Cross Section Schematic of 5 x 10 cm Conditioning Wind Tunnel

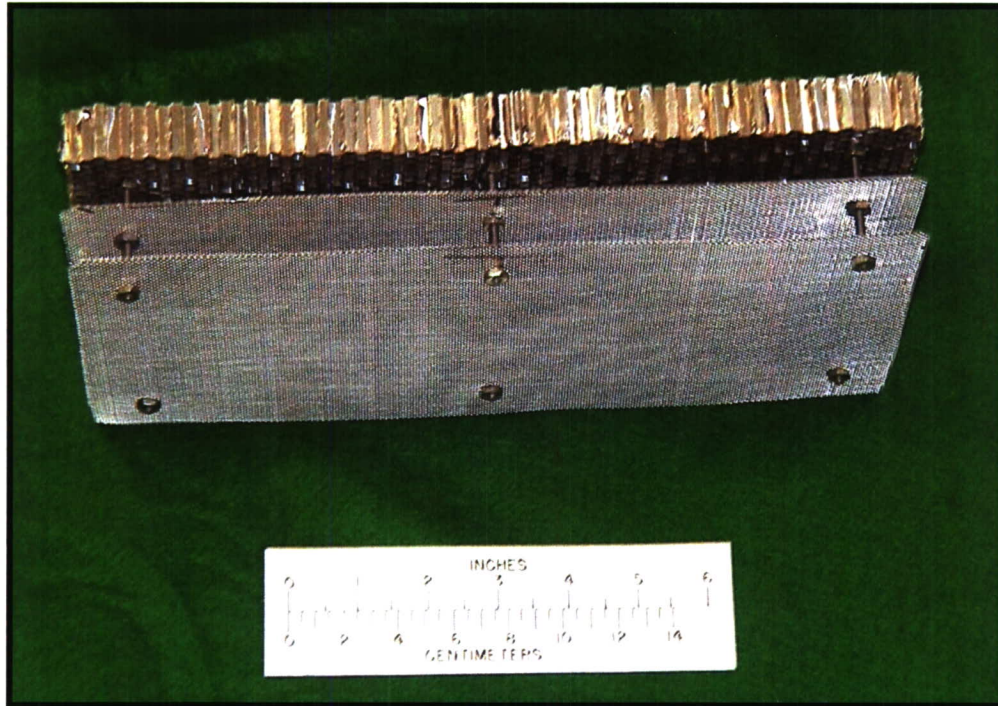


Figure 13. Flow Straightener

3.1.3 Settling Chamber and Contraction Section.

Unlike the 5 cm Agent Fate Wind Tunnel, which used a diverging inlet section, the 5 x 10 cm Conditioning Wind Tunnel used a conventional contraction to supply air to the fetch upstream of the test section. For the Conditioning Wind Tunnel, the settling chamber and the contraction section were manufactured as one piece. The contraction section was intended to smoothly transition from the large cross-sectional area of the settling chamber to the smaller test section cross-sectional area. The contraction ratio (ratio of the contraction's inlet cross section area to the contraction's exit cross-section area) should be as large as possible. Maximizing the settling chamber cross sectional area reduces the air velocity and total pressure drop across the honeycomb and screens. However, maximizing the contraction ratio is normally limited by available space.

According to Bradshaw and Mehta⁷, it is good practice to match the ratio of the contraction section inlet and exit radii to the ratio of the inlet flow width to exit flow width. A spreadsheet was created to study the effects on the top view tunnel contour through the variation of several tunnel design parameters (e.g., test section height and length, contraction ratio and inlet radius and fetch length) to examine the effect on the tunnel layout. A graphical representation of the tunnel contour (top view) was provided to assist in visualizing the effects of the different parameters, see Figure 14.

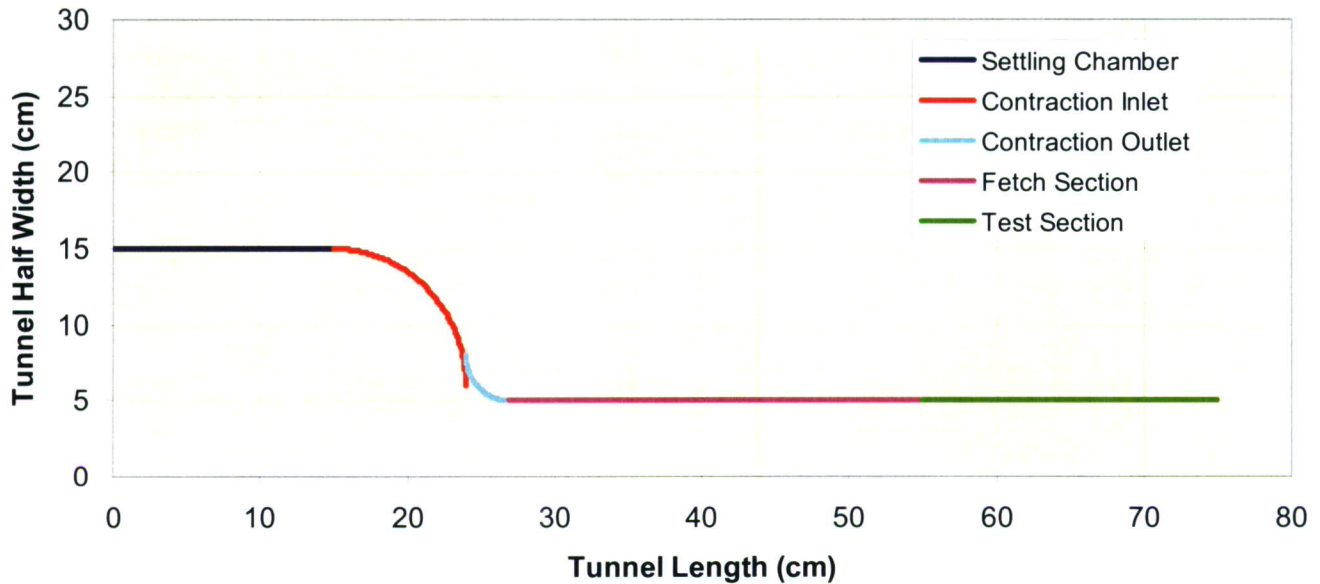


Figure 14. Design Spreadsheet Top Contour View of Conditioning Wind Tunnel

The following values were selected for the tunnel design parameters. The test section height and length were selected as 5 and 20 cm, respectively. The contraction ratio was chosen to be 9 and the contraction inlet radius as 9.0 cm. This produced an overall tunnel length of 75 cm (not including the plenum chamber).

The settling chamber/contraction section was fabricated using rapid prototyping out of plastic and then nickel coated. The nickel coating added structural integrity and provided a more cleanable surface over the uncoated plastic. The coating also diminished the potential for agent being absorbed into the plastic. Figure 15 shows a photograph of the settling chamber/contraction section. The upstream side of this section slipped over a matching protrusion on the plenum section that housed the flow straightening elements. The downstream side of the contraction section incorporated a flange for mating to the fetch section. A future modification would be to equip both ends with flanges to facilitate assembly and provide a positive seal.

3.1.4 Fetch Section and Roughening Elements.

The fetch, test section, and exit sections were fabricated as a single unit comprised of four machined, 1.27 cm thick stainless steel plates. The four plates were assembled with screws and their mating surfaces using a linear O-ring groove to provide a gas tight seal. Although considered one assembled unit, the fetch section, test section and exit section will be discussed separately.

Fetch is a meteorological term referring to the upwind surface area that affects the meteorological conditions at a downwind location. With respect to an environmental wind tunnel, the fetch is the area upwind of the test section. Typically, it is desired that the fetch floor be made from the same substrate material that is being

tested in the test section, such as concrete, sand, asphalt, or some other material. Also, the fetch should be of sufficient length to establish a test section boundary-layer that is representative of the outdoor conditions being simulated. However, wind tunnels used to study the evaporation of highly toxic chemicals impose physical limits on the fetch length. To compensate for this, roughening elements were used to introduce turbulence into the boundary-layer and thereby produce the same effect as a longer fetch.

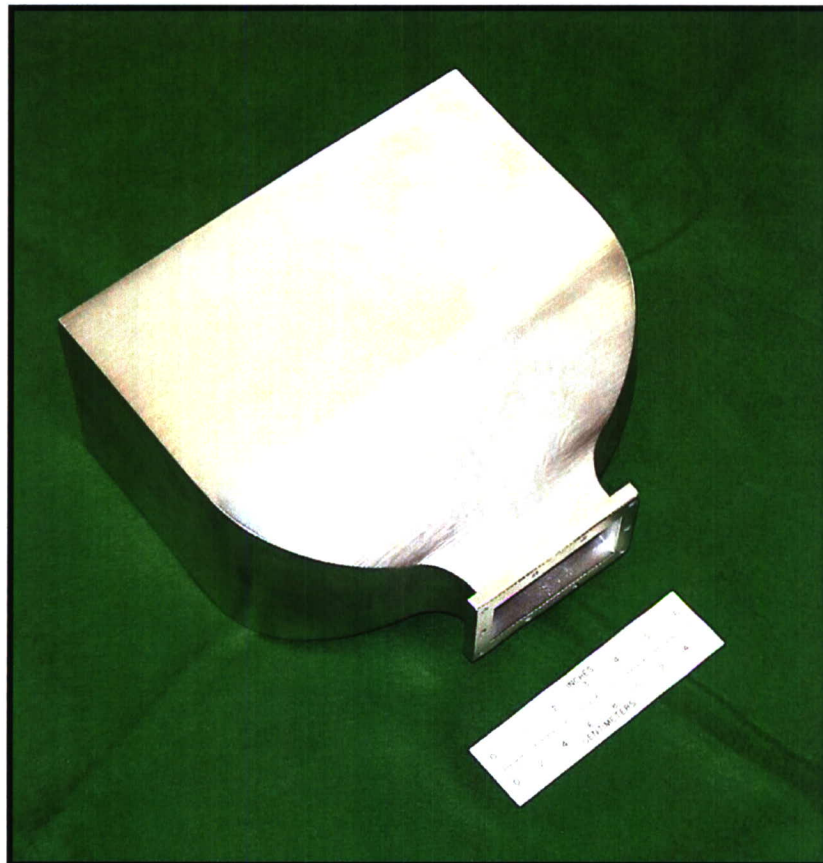


Figure 15. Settling Chamber and Contraction Section

The use of some type of roughening elements is standard practice in larger environmental wind tunnels. The roughening elements add turbulent energy into the boundary-layer, thus shortening the required fetch length needed to generate the desired test section boundary-layers.

The roughening element support consisted of 60 small 4.8 x 4.8 mm square by 2.4 mm high rectangular prisms mounted on a thin plate measuring 9.6 x 9.6 cm square. Identical plates were mounted on the floor and ceiling at the entrance to the fetch section. This arrangement provided symmetrical turbulence generation in the vertical plane containing the measured boundary-layers in the test

section. For the prototype Conditioning Wind Tunnel, the blocks were fabricated from Teflon. A future modification would have the roughening elements machined from a 6.2 mm thick stainless steel plate, which would be mounted into recesses in the fetch, so that the base of the prisms would be flush with the floor and ceiling. Sketches of the fetch section and roughening elements are shown in Figure 16.

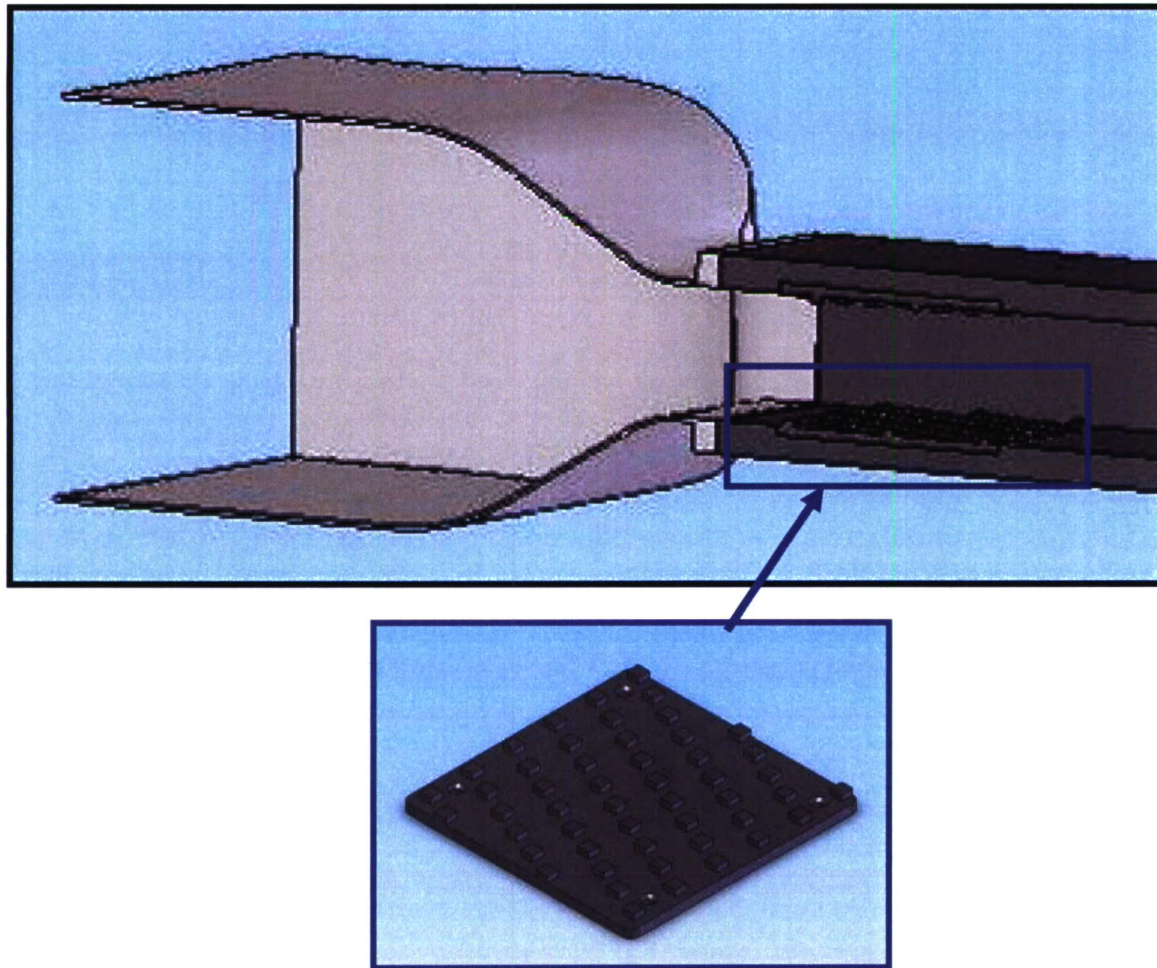


Figure 16. Fetch Section with Roughening Elements

For the Conditioning Wind Tunnel, the roughening element used about a third of the fetch's overall length. The remaining two-thirds of the fetch length downstream of the roughening elements provided time for some of the turbulent energy introduced in the flow to dampen and stabilize creating, better flow homogeneity throughout the test section.

3.1.5 Test Section.

The test section design provided the main impetus for the Conditioning Wind Tunnel and allowed the simultaneous conditioning of eight 3.8 cm diameter test

specimens from the 5 cm Agent Fate Wind Tunnel. The test section floor, containing the eight sample holders in two rows of four, is an independent component that could be lowered from the tunnel and slid forward to remove and load samples. Figure 17 shows the two configurations of the wind tunnel, the test section floor installed (top) and lowered (bottom). A scissor screw type laboratory jack was used as a means of lowering and raising the test section floor. The lowered configuration (Figure 17, bottom picture) has the jack removed to improve clarity. Normally, the jack would be secured to the base plate, preventing safety problems that may occur while lowering the floor and taking out a sample.

All eight substrate holders can be independently adjusted to accommodate differences in thickness of the individual substrates. This permitted the top surface of the substrate to be aligned flush with the test section floor. The holder adjustment mechanism also includes a push rod to assist with substrate removal.

The four plates that form the fetch test and exit sections of the Conditioning Wind Tunnel are shown in Figure 18. The front wall has a window in the test section area for a side view of the test specimens. The top plate or ceiling incorporates two viewing ports above four specimens each. It also includes three access ports, spaced laterally 2.3 cm apart, at the center of the test section for velocity profile surveys and as instrumentation ports during testing. The bottom plate or test section floor has a large rectangular cut-out that allows insertion of the specimen holder/test section floor. The back wall of the test section includes three vertical rows of three holes each to provide access to the test section for additional instrumentation. Each vertical row of holes is centered on the test section half height and with one hole each, spaced 1.4 cm above and below the center hole. The vertical rows of holes are centered lengthwise on the test section, and spaced 9.7 cm fore and aft of the center row.

Ample viewing area is provided by the two windows located in the test section ceiling and the test section side wall. These windows allow observation of the specimens throughout the test without removing them from the test section. The windows also permit digital video filming of the evaporation process for later analysis of the change in droplet shape, volume and contact angle with time.⁸

The test floor was designed to accommodate different size substrate holders, such as different sizes, shapes and quantities, or even a single substrate for possible future multi-drop experiments.

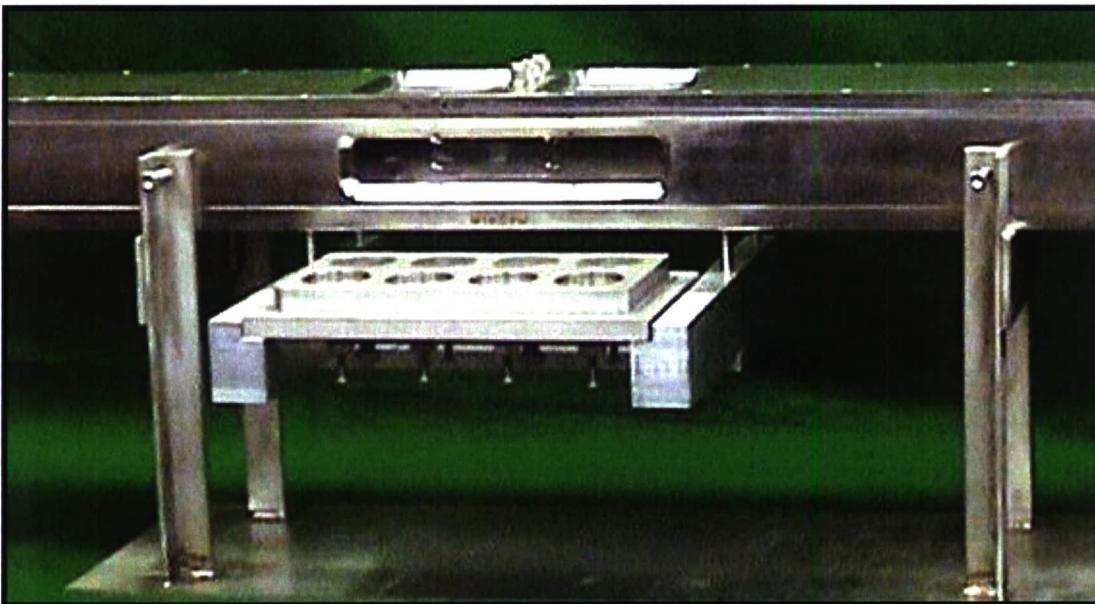
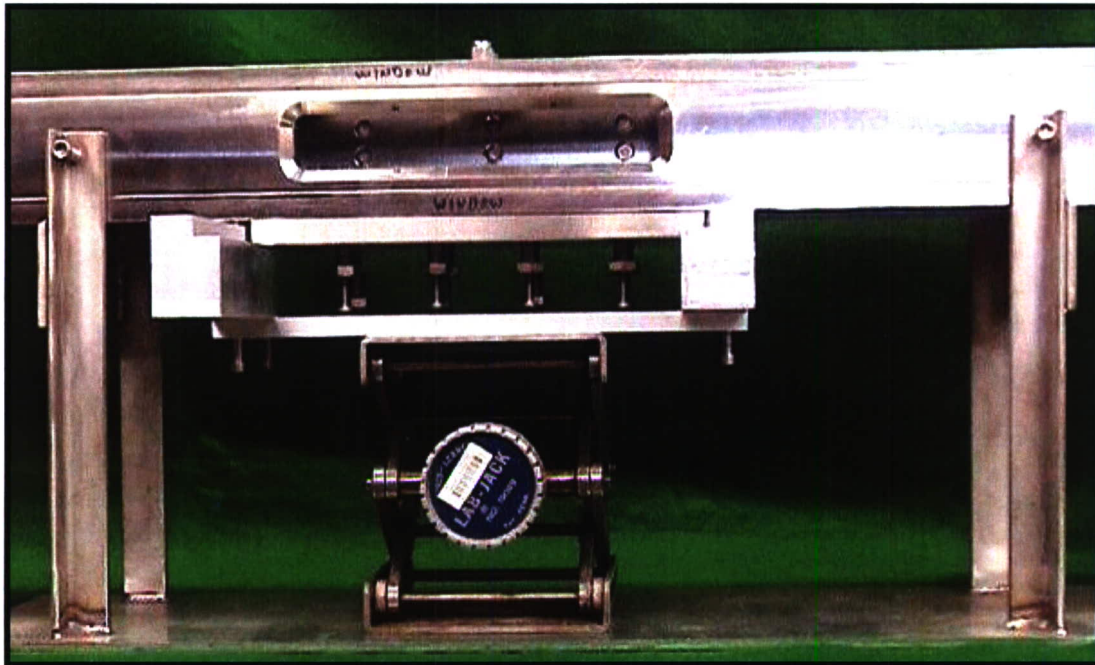


Figure 17. Test Section Floor Installed (top) and in Lowered Position (bottom)

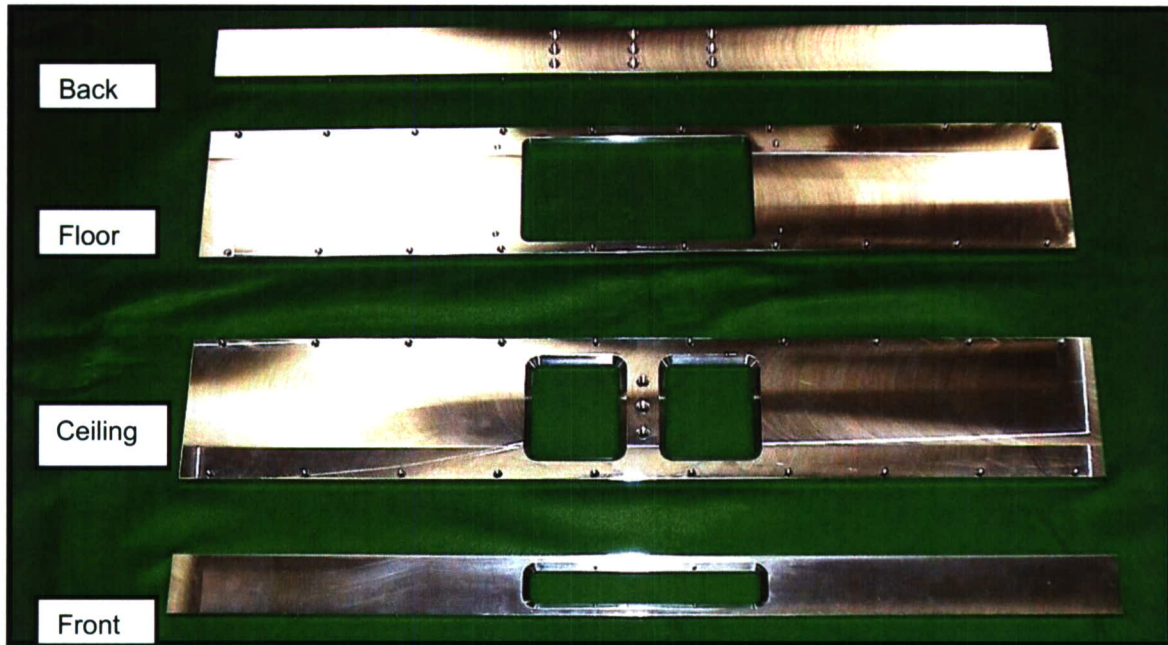


Figure 18. Fetch, Test, and Exit Section Components

3.1.6 Exit Section.

The exit section was positioned just downstream of the test section. The main purpose of this section was to provide sufficient distance to reduce upstream propagation of any disturbances from the exhaust turning vane at the end of the tunnel that might adversely affect the flow in the test section.

3.1.7 Turning Vane Section.

The final component of the Conditioning Wind Tunnel was the turning vane section. Because the Conditioning Wind Tunnel was to be used in a chemical fume hood and the exhaust air would be contaminated with hazardous chemical agent vapor, it was desired to direct the exhaust air upward directly into the fume hood exhaust. The turning vane section relied on two internal turning vanes to smoothly transfer the tunnel airflow from a horizontal to vertical direction. A flange on the turning vane section permitted it to be mounted to the end of the test section. The turning vane section is shown in Figure 19.



Figure 19. Turning Vane Section

3.1.8 Sealing.

Due to the hazardous materials being tested, an airtight tunnel structure was required to assure that no harmful vapor would escape from anywhere along the tunnel except the exhaust. Thus, sealing all joints was vital. Throughout the tunnel, a chemical resistant gasket material, Kalrez[®], was used to seal all mating flange surfaces. A linear O-ring made of Ethylene Propylene rubber was fitted into a small groove that ran the length of the test section plates and around each window in the test section to seal the mating surfaces.

3.1.9 Environmental Conditioning and Instrumentation.

The focus of this report is on the design, flow characterization, and analysis of the velocity profiles for the 5 x 10 cm Conditioning Wind Tunnel. However, to be a fully functioning Conditioning Wind Tunnel, consideration must also be given to controlling the environmental conditions (i.e., temperature, pressure, mass flow rate, and humidity) of the air flowing through the tunnel. An environmental conditioning unit would supply air to the tunnel at the appropriate test conditions. The exterior of the wind tunnel would be wrapped with electrical heat tape and Peltier devices or a water jacket to control the tunnel floor, ceiling and side wall temperatures. These would maintain the desired airflow temperature and minimize condensation of the agent vapor on the tunnel internal surfaces. In addition, the tunnel will require a full set of

instrumentation to monitor control airflow, temperature, and humidity in the wind tunnel, as well as a number of sensors to measure and control tunnel ceiling, floor, and side walls temperatures. As noted previously, no vapor measuring instrumentation would be present.

3.2 Conditioning Tunnel Flow Field Characterization.

The procedures followed in characterizing the flow in the 5 x 10 cm Conditioning Wind Tunnel were similar to those used in the characterization of the 5 cm Agent Fate Wind Tunnel.⁴ However, due to the larger test section size of the Conditioning Wind Tunnel, some modifications to the characterization procedures were required. Doubling of the test cross-sectional area caused a doubling of the flow rate required to produce the operational profiles. This required a larger air source and mass flow controller than the Miller-Nelson[®] (Model HCS-401, Miller-Nelson Research, Monterey, CA) air conditioning units used to characterize the 5 cm Agent Fate Wind Tunnel. A large in-house air compressor system capable of supplying dry filtered air was used as the air source. A 1,000 L/min Aalborg mass flow controller was used to control the airflow rate from the house air supply to the tunnel's plenum. All testing was performed at room temperature of approximately 25 °C. The velocity profile characterization test setup is shown in Figure 20.

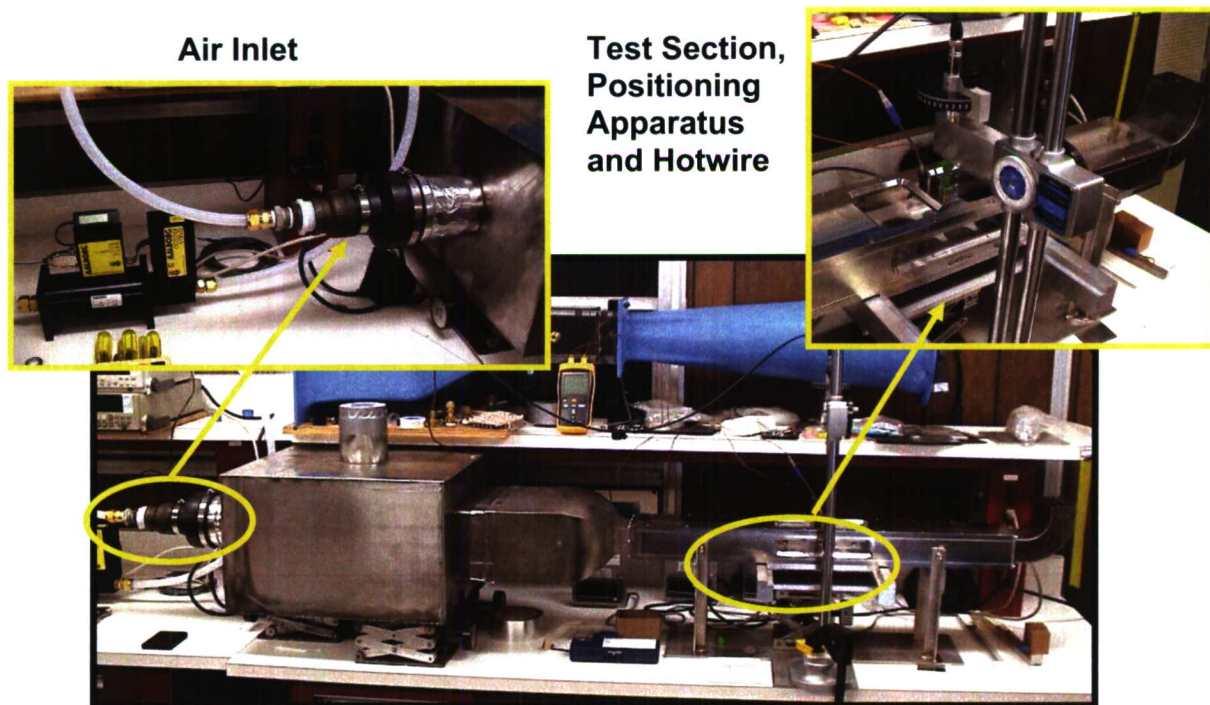


Figure 20. Velocity Profile Characterization Test Setup

For the Agent Fate Program, three operational velocities, 0.5, 3.0 and 6.0 m/s at a height of 2 m were prescribed. These profiles were extrapolated down to the ground using turbulent boundary-layer theory. Because of the difficulty in

establishing the low flow rate required for the 0.5 m/s and the concern that the smooth surface, turbulent boundary-layer theory may not be applicable for this condition, the Conditioning Wind Tunnel was only characterized at the medium (3.0 m/s) and the high (6.0 m/s) flow conditions. The airflow rate through the tunnel was adjusted so that the measured centerline velocity at 0.5 cm above the tunnel floor matched the operational profiles at the same height. The velocity at 0.5 cm was set at 1.42 m/s and 3.00 m/s for the mid and high velocities, respectively. (The corrected operational profiles 0.5 cm velocities for the medium and high velocities were 1.44 and 3.04 m/s, respectively. Within measurement error, the original and corrected velocities were essentially equal.) In each case, once set, the flow rate was held constant and velocity profiles measured using a single component hot film anemometer through the three ceiling ports in the center of the test section.

The Conditioning Wind Tunnel velocity profiles corresponding to the medium operational velocity condition are shown in Figure 21. The prescribed operational profile for the medium velocity condition (3.0 m/s at 2 m) is indicated by the red curve. The other four curves represent two profiles taken at the center port and one profile each from the left and right ports. Visually, the agreement with the operational profile is good below 0.5 cm, which is near the agent/substrate and the area of most interest. The four profiles deviate from the operational profile above 0.5 cm, which is to be expected because of the duct like flow of the wind tunnel and the effects of the ceiling boundary layer. It should be noted that the operational profiles depicted in this report are slightly different from past reports due to an error that was discovered and corrected in the application of the wake term in the development of the operational profiles.

The results of the velocity profile characterization of the Conditioning Tunnel for the high wind speed condition (6.0 m/s at 2 m) are presented in Figure 22. As before, the operational profile is shown in red and is compared with the three measured profiles, one at the center and the other two, one right and the other left of center, respectively. The results were similar to the medium velocity case in that the agreement of the high speed velocity profiles with the operational profile was good below 0.5 cm. Above 0.5 cm the measured profiles departed from the operational profiles, again due to effects of duct flow and the ceiling boundary-layer.

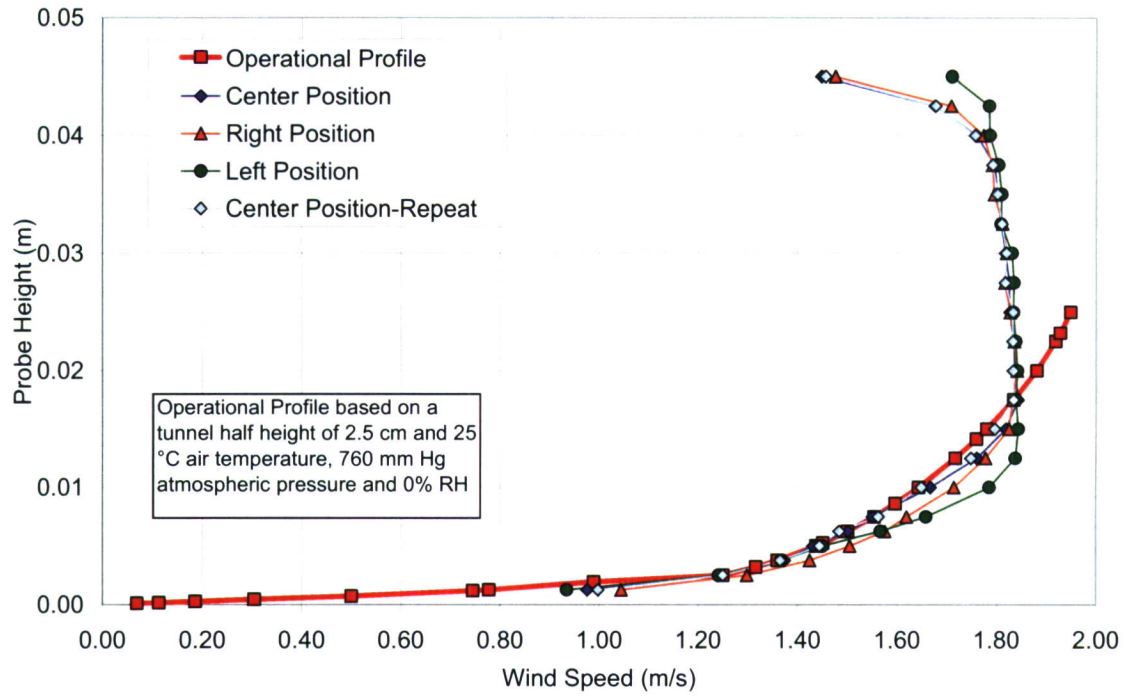


Figure 21. Velocity Profile Characterization, Medium Velocity Case

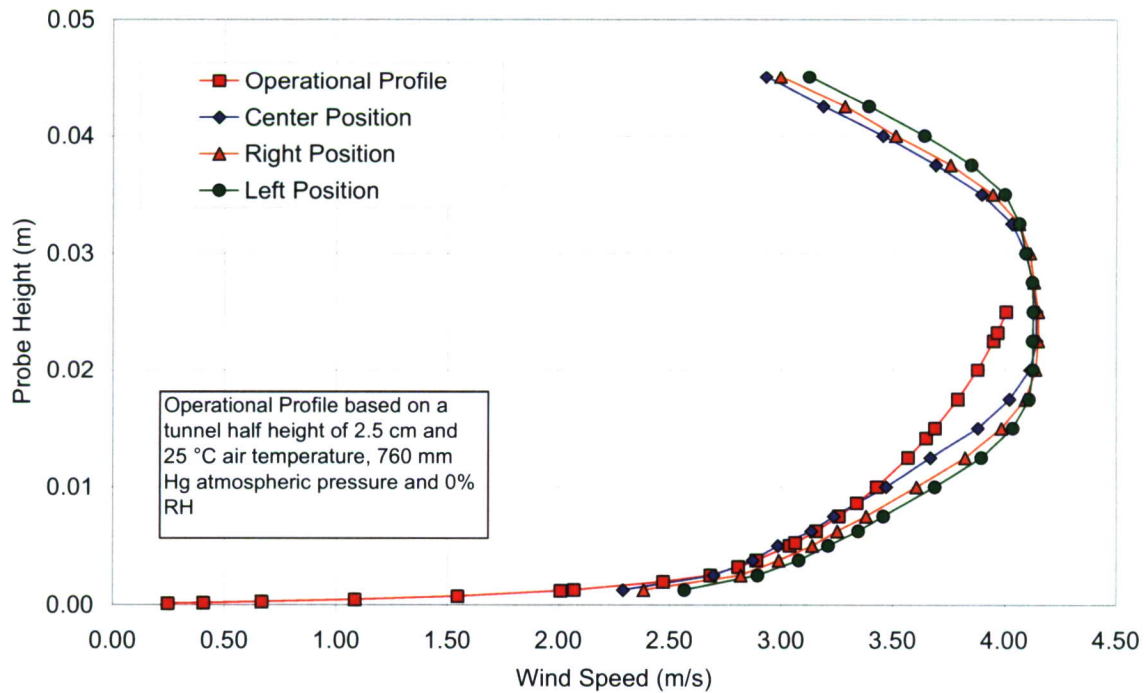


Figure 22. Velocity Profile Characterization, High Velocity Case

4. VELOCITY PROFILE ANALYSIS

Instead of relying only on visual confirmation of the profiles that were in good agreement with the prescribed “operational” profiles, two analyzes were performed to quantify the agreement. The first analysis was a preliminary check on how well the profiles agreed with the operational parameters. The second analysis was more detailed and in depth and included wake parameters.

The smooth wall turbulent boundary layer equation used to extrapolate the 2 m height velocity to the surface is referred to as the logarithm law or “log-law” for short. This equation can be used to analyze the measured profile data.

4.1 Regions of a Fully Developed, Equilibrium Turbulent Boundary Layer.

Historically, turbulent boundary layers have been divided into four main regions: a laminar sub-layer, buffer or transition layer, the logarithmic (log-law) region, and a wake or defect region.⁹ An atmospheric boundary layer and the operational profile that is intended to model such a case do not have a wake region but wind tunnel velocity distributions do, and thus, the wake requires some consideration. These regions are illustrated in Figure 23.

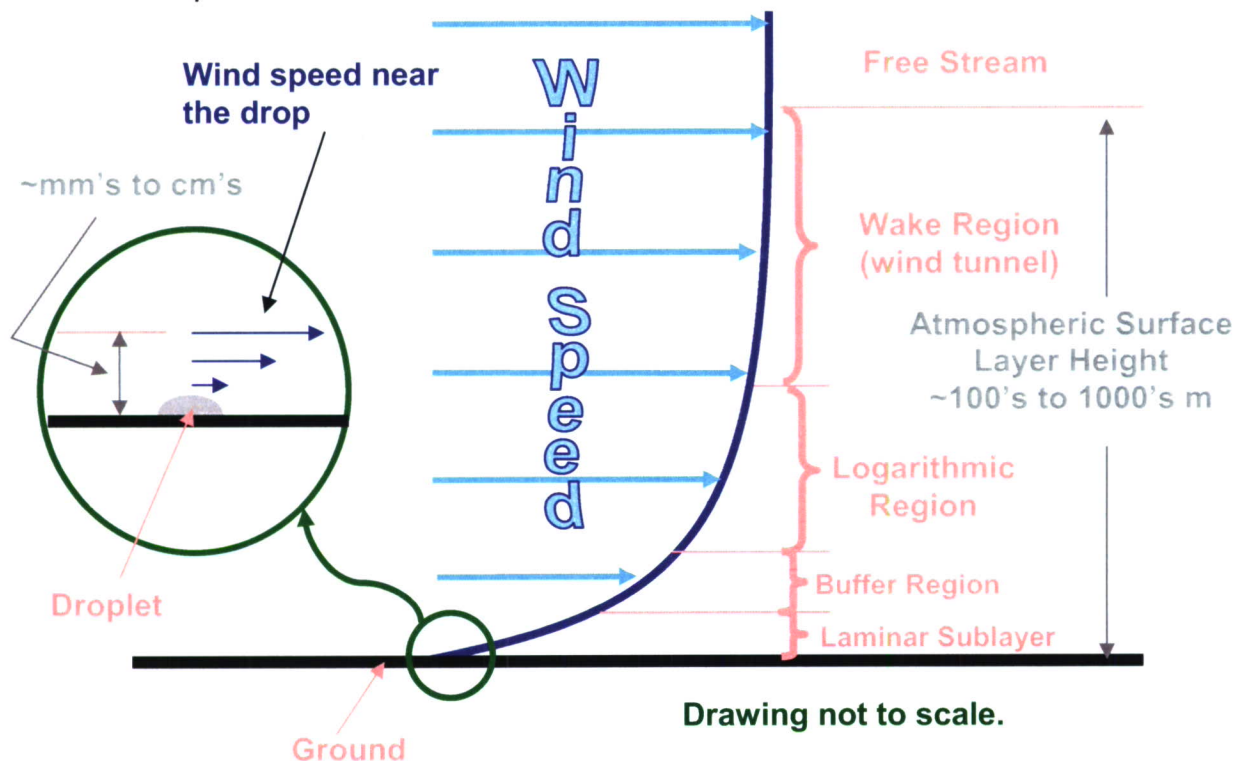


Figure 23. Regions of the Turbulent Boundary-Layer

Laminar sub-layers extend a short distance from the surface, and at the surface, satisfy the “no-slip” boundary condition required of viscous fluids. It is assumed that the zero velocity condition also applies on the evaporating liquid agent because of its high density and inertia. Typically the chemical agent droplet will be confined to the laminar sub-layer. In this region, molecular viscosity dominates. Although the extent of the layer is imprecisely defined, there must be a transition from this molecular viscosity layer to a turbulent motion dominated layer. Molecular and turbulent viscosities are important in the buffer layer. In the “log-law” region, turbulent mixing creates an effective viscosity, which dominates over molecular viscosity. This results in the characteristic behavior of the velocity where it becomes proportional to the logarithm of y , the height above the surface.

4.2 Logarithmic-Region.

The logarithmic region is so named because the velocity is linearly proportional to the log of the height as given by eq 1.

$$u \propto \ln(y) \quad (1)$$

It has been found that eq 1 takes the following form of eq 2, which is referred to as the “log-law”.

$$\frac{u}{u_\tau} = \frac{1}{\kappa} \cdot \ln\left(\frac{u_\tau y}{\nu}\right) + C \quad (2)$$

Where κ is the von Karman Universal Constant of Turbulence and is $\cong 0.4$, ν is the air’s kinematic viscosity and u_τ is the friction velocity given by eq 3. In the wall layers the friction velocity, u_τ , provides a velocity scale, and ν/u_τ is the appropriate length scale. When the velocity and y are made non-dimensional by their scales they are designated by u^+ and y^+ .

$$u_\tau = \sqrt{\frac{\tau_w}{\rho}} = \sqrt{\nu \left(\frac{\partial u}{\partial y} \right)_w} \quad (3)$$

The friction velocity is a function of the shear stress, τ_w , at the surface caused by the air moving over the surface. The constant, ρ , is the density of the air.

4.3 Operational Profile.

Equation 2 has been used to model three atmospheric surface layers by assuming three values for the friction velocity $u_\tau = 0.020$, 0.104 , and 0.197 m/s, creating the “operational” velocity profiles.⁵ These values correspond roughly to velocities of 0.5 , 3.0 , and 6.0 m/s at a height of 2 m. In Equation 2, values of $\kappa = 0.4$ and $C = 5$ were

assumed, and v was calculated based on air temperature, pressure, and humidity of the experiment. As mentioned previously, only medium and high velocity cases were characterized in this study.

5. MEASURE VELOCITIES COMPARED TO “OPERATIONAL” PROFILE

The main purpose of the velocity analysis was to determine how well the velocity profile measurements matched the “operational” profiles, especially around the sessile droplets or absorbed agent near the tunnel floor. This comparison relies on the agreement between the calculated friction velocities from the measured profiles and the corresponding “operational” profile friction velocities. A secondary purpose of the analysis was the experimental determination of a wake constant to ascertain how close the flow in the Conditioning Tunnel was to an equilibrium turbulent boundary layer.

A good means of highlighting the logarithmic region of the boundary layer is by plotting the velocity profiles as a function of $\ln(y)$. In this form, the laminar sub-layer appears as a curve and the logarithmic region appears as a straight line, and their intersection is the transition region. The Conditioning Tunnel medium and high velocity profile cases are shown in Figures 24 and 25, respectively.

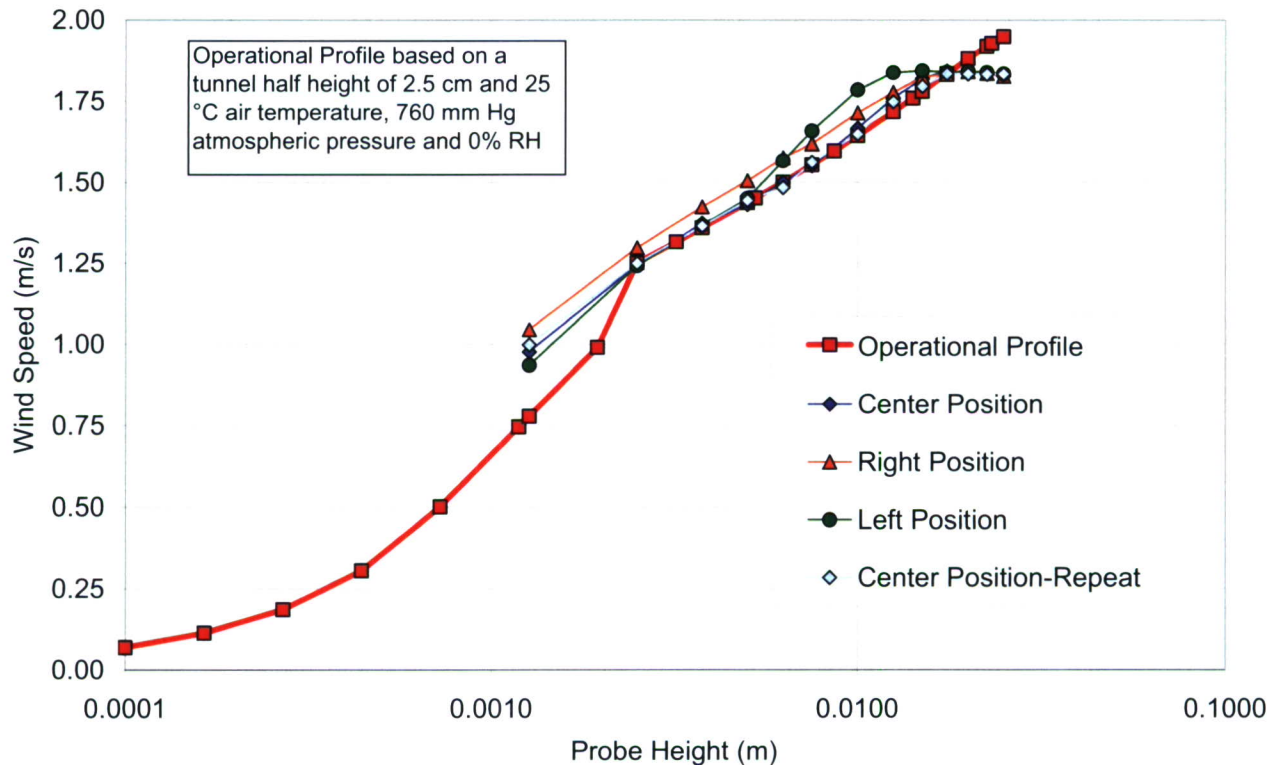


Figure 24. Medium Velocity Profile, Velocity vs. $\log(y)$

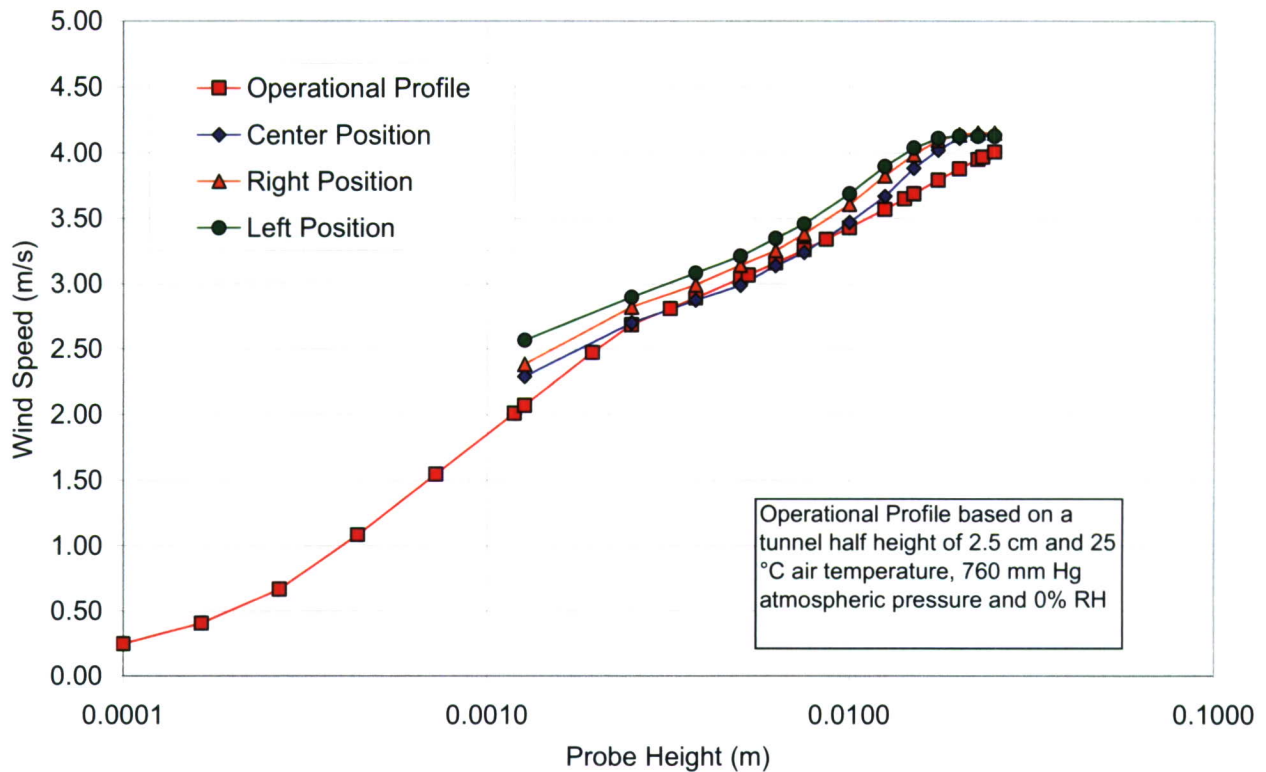


Figure 25. High Velocity Profile, Velocity vs. Log(y)

As can be seen in Figures 24 and 25, the lowest velocity measurements deviate from the transition to the laminar sub-layer. This is most likely due to a heat transfer phenomenon between the hotwire and the tunnel floor, causing a higher indicated wind speed than is actually present. Also, velocities near the center of the tunnel deviate from the “operational” profile due to the boundary layer wake that in channel flow is due to a transition to the boundary layer formed by the tunnel ceiling. The left and right profiles show influence from the boundary layers coming off the tunnel side walls.

Determining u_τ and “Log-Law” from Velocity Measurements.

To determine the friction velocity from the experimental measurements, a least squares fit of the data was performed on a selected number of data points in the logarithmic region. Typically, the first measurement of each profile was excluded from the curve fit, and the next five data points were used. A linear regression analysis provided the curve fits shown in Figures 26 and 27 for the medium and high velocity cases, respectively.

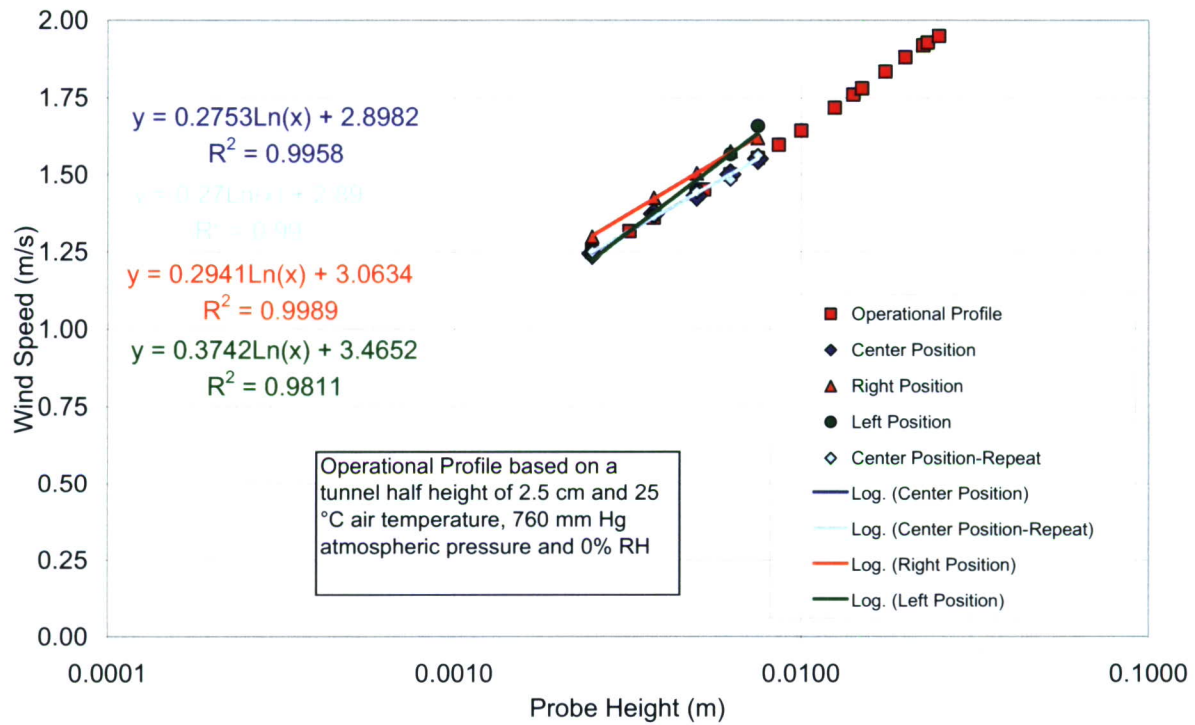


Figure 26. Least Squares Curve Fit of Medium Velocity Profiles (5 points)

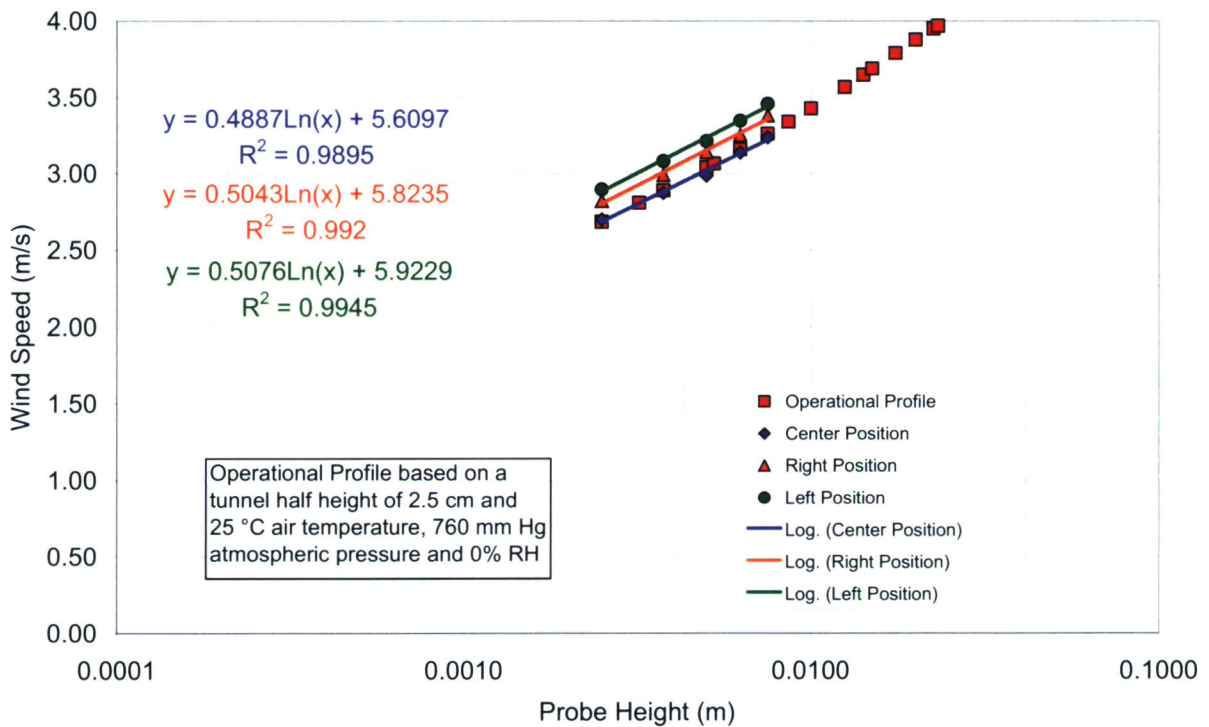


Figure 27. Least Squares Curve Fit of High Velocity Profiles (5 points)

From the linear regression analysis a straight line is obtained for each of the profiles in the logarithmic region. The curve is of the form, $u = b \ln(y) + a$, where the slope of the line is directly proportional to the friction velocity, $u_\tau = \kappa b$. With u_τ known, the constant C in eq 2 can be determined by eq 4:

$$C = \frac{a}{u_\tau} - \frac{1}{\kappa} \ln\left(\frac{u_\tau}{v}\right) \quad (4)$$

Calculated values of u_τ and C for the medium and high speed profiles are shown in Table 1. Overall, the higher wind speed measured profiles parameters were in better agreement with those of the “operational” profile than the medium case. Within the respective velocity conditions, the centerline profiles show very good agreement between the calculated and selected “operational” friction velocities and constant C. The poorest agreement is for the medium velocity, left profile with the right profile showing fair agreement. A reason for the medium velocity side profiles showing less than good agreement is related to the growth of the side wall boundary layers. This effect can be seen in the higher measurements of the logarithmic region in the medium side profiles. The calculated uncertainty for the parameters u_τ and C are with respect to the nominal “operational” profile values.

Table 1. Conditioning Tunnel Linear Regression Analysis Results

Wind Speed (m/s) at 2m	Profile	Log Region Curve Fit				Operational Profile		%Δ U_τ	%Δ C
		Slope	y-intercept	U_τ (m/s)	C	U_τ (m/s)	C		
Medium 3.0	left	0.37	3.47	0.15	0.23	0.104	5	43.9	-95.5
	center	0.28	2.90	0.11	4.16			5.9	-16.7
	center repeat	0.27	2.89	0.11	4.65			3.8	-7.0
	right	0.29	3.06	0.12	3.72			13.1	-25.6
High 6.0	left	0.51	5.92	0.20	5.49	0.197	5	3.1	9.7
	center	0.49	5.61	0.20	5.11			-0.8	2.1
	right	0.50	5.82	0.20	5.20			2.4	4.0

6. “LAW OF THE WAKE” ANALYSIS

Wake regions connect boundary layers to their external free-stream or in the case of internal flow, it connects the viscous layers from opposing walls. It is also a transition layer in that the turbulent motion in the “log-law” adjusts to the turbulence

conditions in the free-stream. Wake regions differ from wall regions in that the total boundary layer thickness, δ , is the important length scaling parameter, although the friction velocity remains the velocity scaling parameter. A unique feature of the wake region is that it also includes the “log-law” region. In this overlap region, both length scales are valid.

In a wake analysis performed on the 5 cm Agent Fate Wind Tunnel profiles, the wake region was not considered of high importance relative to the inner wall region in determining how well the measured profiles matched the “operational” profiles. This was because the evaporation rates of very small droplets are controlled by the inner wall layer and also because atmospheric surface layers do not exhibit a wake region. Friction velocities and the near wall comparisons, based on the measurements, were considered more significant. However, for interpretation of ECBC results in comparison with those of other facilities, it can be important to provide the wake data and analysis.

6.1 Coles’ Wake Function.

Coles’ empirical “Law of the Wake” theory, which accounts for the deviation in velocity from the logarithmic region,¹⁰ has been applied to the current results. Equation (2) can be modified (eq 5) to include a term that approximately describes the velocity distribution in the “log-law” and the wake regions.

$$\frac{u}{u_\tau} = \frac{1}{\kappa} \cdot \ln\left(\frac{u_\tau y}{\nu}\right) + C + \frac{\Pi}{\kappa} \cdot 2 \cdot \sin^2\left(\frac{\pi y}{2\delta}\right) \quad (5)$$

The additional wake parameter Π is based on experimental data. A wake parameter D also can be defined as the difference between the external free stream velocity (centerline velocity for internal flows) and the “log-law” (eq 2) prediction at $y=\delta$. Equation 5 shows that $D=2\Pi/\kappa$ at $y=\delta$, $u=u_\delta$.

6.2 Comparison of Channel Flow Operation Profile with Wake and Experimental Data.

Wake velocity profile measurements are compared to the “operational” profile with Coles wake term in Figures 28 and 29. The wake parameters in these calculations are $D=1.0$ and $\delta=h/2=0.025$ m. These assumptions are consistent with fully developed channel flow.

¹⁰Danberg, J.E., Science Applications International Corporation, Abingdon, MD, Memorandum for Record, 27 November 2006, subject: *Wake Region of 5-cm Agent Fate Wind Tunnel Velocity Profile*

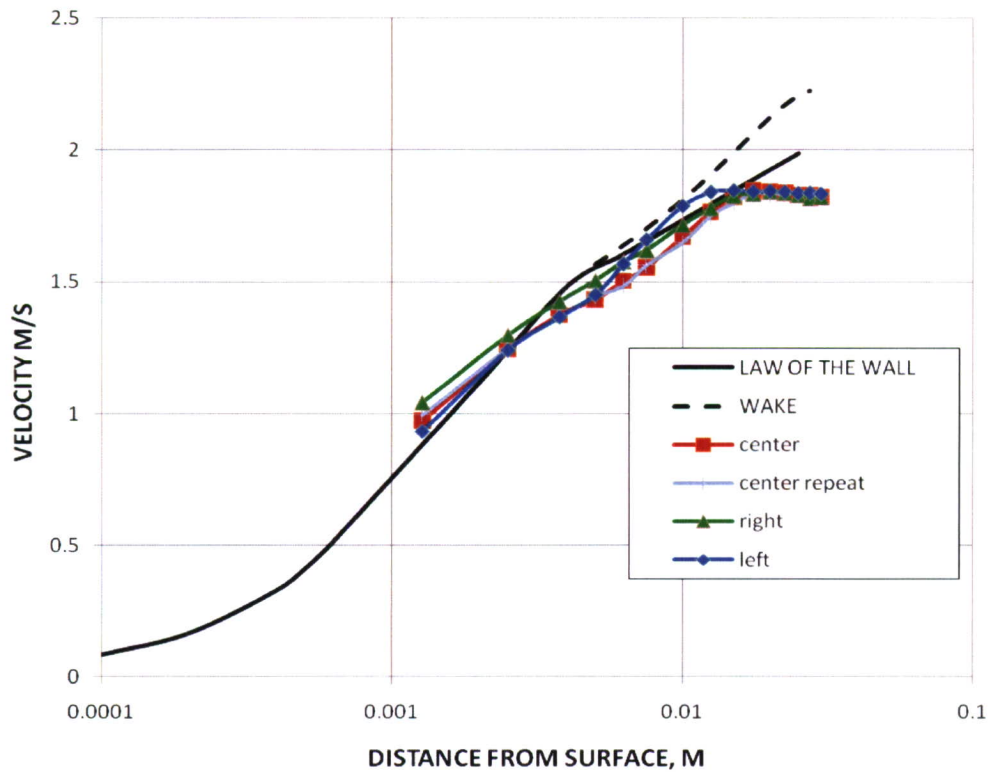


Figure 28. Comparison of Operation Profile with and without Wake to Conditioning Tunnel Data, Medium Wind Velocity

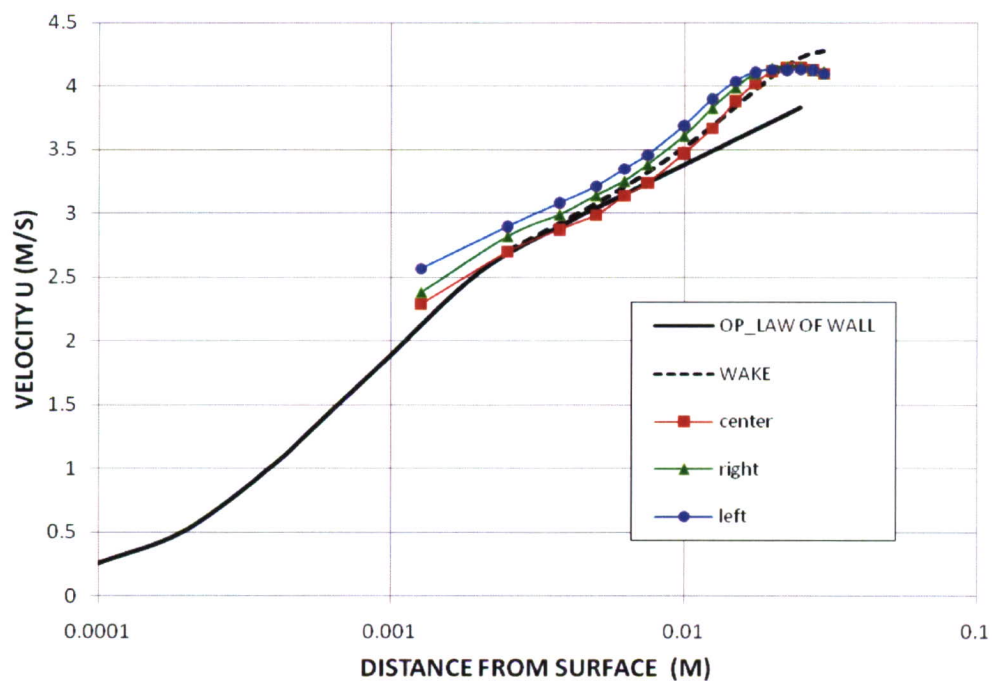


Figure 29. Comparison of Operation Profile with and without Wake to Conditioning Tunnel Data, High Wind Velocity

The “operational log-law” ($C=5$ and $\kappa=0.4$) with channel flow wake ($D=1$ and $\delta= h/2$) somewhat over estimates the velocity for the medium wind speed case and provides a better agreement in for the high velocity case. In both speed cases, the viscous layer thickness, δ , is over predicted by the channel half height.

6.3 Channel Flow.

Taking $\delta= h/2=0.025$ m in calculating the wake does not give a good approximation for the boundary thickness indicating the flow in the tunnel is not fully developed channel flow (high velocity case $\delta \approx 0.02$ m and for medium case $\delta \approx 0.016$ m from estimate of location of maximum velocity). The assumption of fully developed channel flow over predicts the wake for the medium speed cases but it is in much better agreement for the higher speed data. This observation is supported by examining Figures 21 and 22. Figure 21 shows the medium velocity distribution over the height of the test section and exhibits a plateau in velocity from $0.012 < y < 0.04$ m or approximately 56% of the tunnel height. The velocity in this region also has a small gradient indicating the flow is not perfectly symmetrical. The higher velocity case (and higher Reynolds number) is shown in Figure 22. It shows a smaller plateau between $0.02 < y < 0.030$ or 20%.

6.4 Optimum Coles' Wake Function Parameters for Experimental Profiles.

An alternative approach to that of the previous section for comparing the measured profiles to the “operational” profile involves determining the parameters required to provide a fit between Coles' empirical theory and each individual experimental velocity profile. The attempt to determine the friction velocity by least square fit of the “log-law” to a selected sub set of data that is linear in semi-logarithmic format provides an estimate of u_τ and the intercept parameter C . Basically the same result can be obtained by searching for the values of u_τ and C that minimize the sum of the square discrepancies between the velocity predicted by the “log-law” (eq 2) and the measurements. The square deviation between the predicted u_{pi} and measured velocity u_i at y_i is given by R_i as defined in eq 6.

$$R_i = (u_i - u_{pi})^2 \quad (6)$$

Thus, a quantity S is minimized as shown in eq 7.

$$S = \sum_2^7 R_i = \sum_2^7 (u_i - u_{pi})^2 = \sum_2^7 \left\{ u_i - u_\tau \left[\frac{1}{\kappa} \ln \left(\frac{u_\tau y_i}{\nu} \right) + C \right] \right\}^2 \quad (7)$$

The summation is taken over the same (5) (u_i, y_i) data pairs as used in the least square fit. This procedure requires a nonlinear fitting technique.

Examination of eq 5 shows that to include the wake, the majority of the profile data, the boundary layer thickness and Coles wake parameter, Π must be determined. To do this, it is more efficient to put eq 5 into the “Law of the Wake” format. First writing eq 5 for $y=\delta$ produces eq (8).

$$\frac{u_\delta}{u_\tau} = \frac{1}{\kappa} \cdot \ln\left(\frac{u_\tau \delta}{\nu}\right) + C + \frac{2\Pi}{\kappa} \quad (8)$$

Subtracting eq 5 from 8 obtains the “Law of the Wake” as eq 9:

$$\frac{u_\delta - u_{pi}}{u_\tau} = -\frac{1}{\kappa} \cdot \ln\left(\frac{y_i}{\delta}\right) + \frac{2\Pi}{\kappa} \left(1 - \sin^2\left[\frac{\pi}{2} \frac{y_i}{\delta}\right]\right) \quad (9)$$

As in eq 7, u_{pi} is the predicted velocity at a typical measurement location y_i . A square deviation between the predicted and measured velocity u_i at y_i is given by R_i shown in eq 10.

$$S = \sum_2^n R_i = \sum_2^n \left\{ u_i - u_\delta + u_\tau \left[-\frac{1}{\kappa} \ln\left(\frac{y_i}{\delta}\right) + \frac{2\Pi}{\kappa} \left(1 - \sin^2\left[\frac{\pi}{2} \frac{y_i}{\delta}\right]\right) \right] \right\}^2 \quad (10)$$

where the sum is over all the data pairs $(u_i, y_i) \leq \delta$. Assuming u_τ is known from the previous calculation and searching for values of Π and δ , which minimizes the sum S , the results for the seven conditioning tunnel velocity profiles are shown in Table 2[‡].

6.5 Discussion of Table 2 Results.

Values of u_τ and C in Table 2 agree closely with their earlier evaluations except for the medium speed- left profile. For this case, and only this case, the number of points used to determine u_τ and C in Table 2 was reduced from 5 to 3 because of the departure from linearity in the semi-logarithmic coordinates. This improved the medium speed- left parameters relative to the “operational” profile values.

The boundary layer thickness δ is consistent with the maximum velocity u_δ observed from the measured data. It should be noted that the tabulated u_δ values are obtained directly from the measurements and are used as input to the calculations with eq 8.

[‡] Table 2 values of u_τ , C and Π , δ were obtained by using the Solver program in an Excel spread sheet.

Table 2. Conditioning Tunnel Velocity Profile Parameters

RUN	Ctr	Medium Wind Speed			Average
		Ctr-Rep	Right	Left	
Π	0.151	0.075	-0.031	0.257	0.113
δ (m)	0.0168	0.0183	0.0161	0.0122	0.0158
u_τ (m/s)	0.1106	0.1105	0.1178	0.1208	0.115
C	3.97	4	3.59	2.76	3.58
$2\Pi/\kappa$	0.753	0.375	-0.156	1.284	0.564
u_δ (m/s)	1.843	1.834	1.836	1.843	1.84
Re_θ	211	230	201	187	207
RUN	Ctr	High Wind Speed			Average
			Right	Left	
Π	0.466		0.352	0.275	0.364
δ (m)	0.0217		0.0204	0.0185	0.0202
u_τ (m/s)	0.1975		0.2033	0.2041	0.202
C	4.97		4.94	5.27	5.06
$2\Pi/\kappa$	2.33		1.76	1.38	1.82
u_δ (m/s)	4.143		4.172	4.136	4.15
Re_θ	666		597	557	607

One conclusion drawn from the tabulated values of Π and C is that the viscous layer is not in equilibrium. This is because of the very low Reynolds number and the developing channel inlet conditions. Values of the momentum thickness Reynolds number in Table 2 are based on $u_\delta \theta / \nu$, where θ is an integral of local flux of momentum. This Reynolds number is often used to characterize the upstream history of the viscous region when the origin of boundary layer is unknown.

The value of the wake parameter is higher than expected for the high wind speed case. Comparison of the current wake results can be made with a number of sources in the form of Π or $D=2\Pi/\kappa$. Pipe¹¹ and channel¹² flows are generally found to have $D=0.65-1.0$, whereas the experimental data cited for external zero pressure gradient boundary layers give $D=2.3-2.5$ ^{122,13}, although Coles $\Pi=0.55$ for momentum thickness Reynolds numbers $Re_\theta > 5000$ corresponds to a $D=2.75$. Coles^{100, 14} showed that Π decreased at low Re_θ and $\Pi \approx 0$ at $Re_\theta \approx 425$. Because the current medium speed case $Re_\theta = 200$, it is expected to have a minimum wake layer. The estimated high wind speed value of $\Pi \approx 0.47$ is substantially greater than predicted by Coles, although the tripping roughness in the inlet may have an effect on results from both wind speeds.

Figure 30 illustrates the good quality of the fit equations and centerline measured profiles at both speeds. At the higher wind speed, the velocity is slightly over predicted indicating that the wake term decreases faster in the experiment than in the fit equation.

$$\begin{aligned}
0 \leq y^+ < 5.0 & \quad u = \frac{u_\tau^2 y}{\nu} \\
5.0 \leq y^+ < 30.0, & \quad u = u_\tau \left[(1.96 + 0.56C) \cdot \ln \left(\frac{u_\tau y}{\nu} \right) + (1.85 - 0.9C) \right] \\
30.0 \leq y^+ \text{ \& } y \leq \delta & \quad u = u_\tau \left[\frac{1}{\kappa} \cdot \ln \left(\frac{u_\tau y}{\nu} \right) + C + \frac{\Pi}{\kappa} \cdot 2 \cdot \sin^2 \left(\frac{\pi y}{2\delta} \right) \right]
\end{aligned} \tag{11}^\S$$

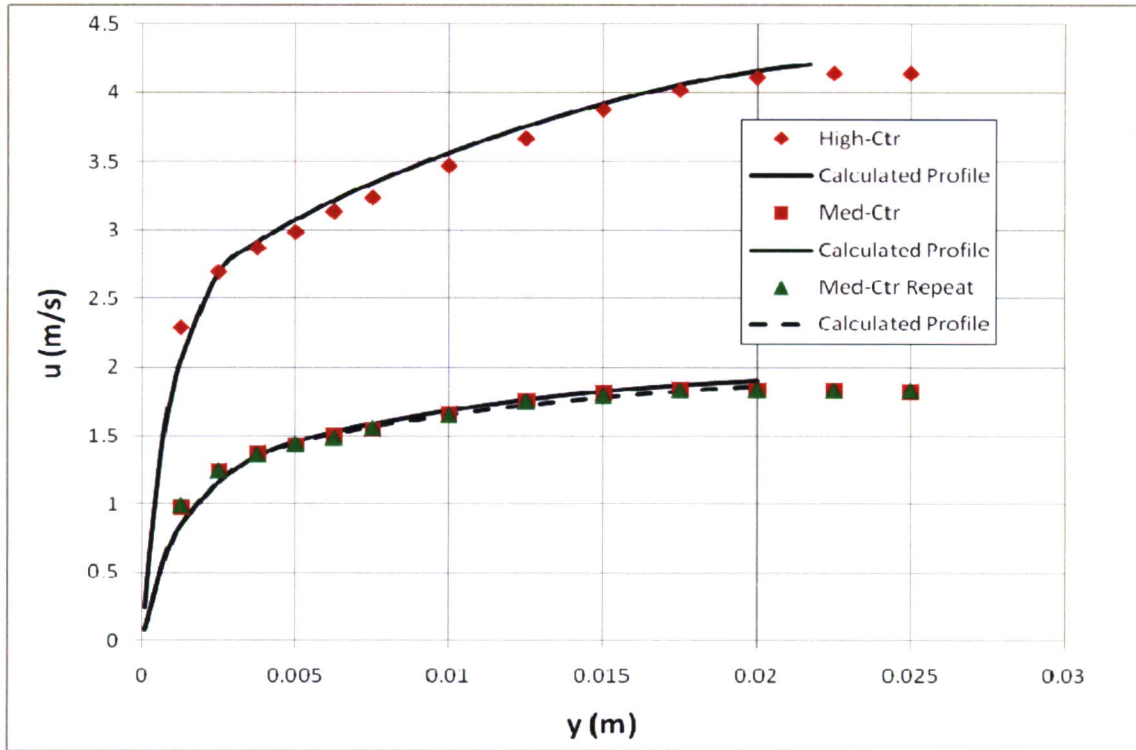


Figure 30. Comparison Between Predicted Law of the Wake and Centerline Velocity Measurements for High and Medium Speed Conditions

Figures 31 and 32 compare the measured velocity profiles with a composite “Law of the Wall” profile based on the average profile parameters. The Law of the Wall is constructed as follows (eq 11) with a non-dimensional height defined as $y^+ = u_\tau y / \nu$.

[§] The buffer layer formula is based on the assumption that the velocity is proportion to $\ln(y^+)$ between the sublayer at $y^+ = u^+ = 5.0$ and the Log-Law at $y^+ = 30$ with different values of C.

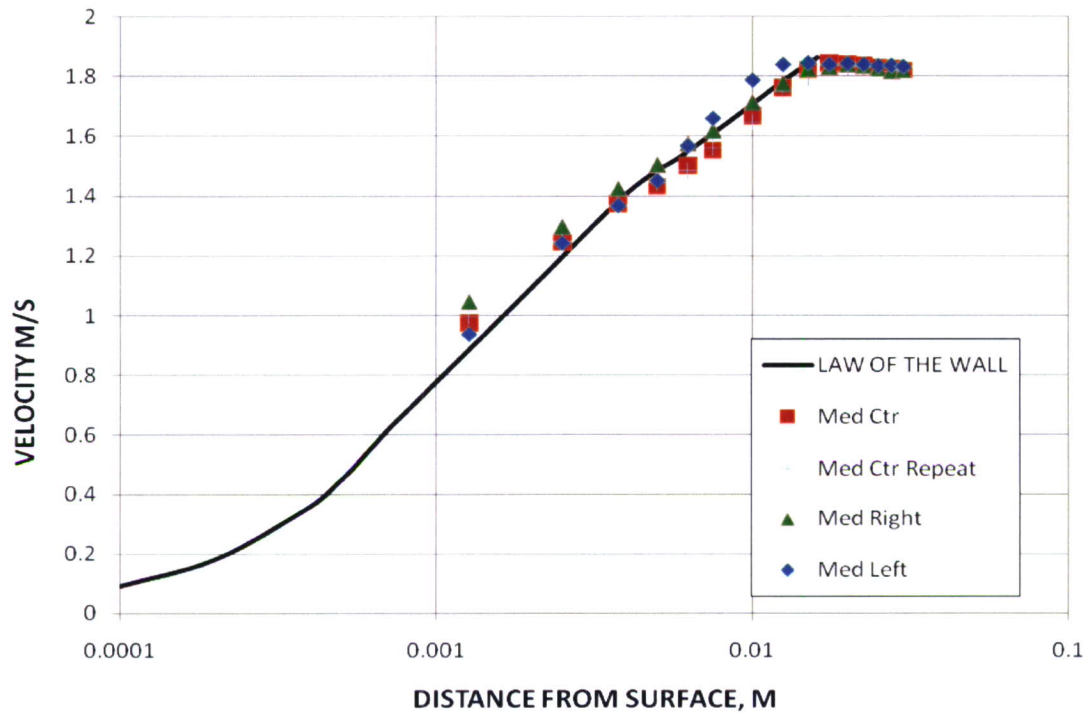


Figure 31. Comparison Between Predicted Law of the Wake Based on Average Parameters and Medium Wind Speed Data

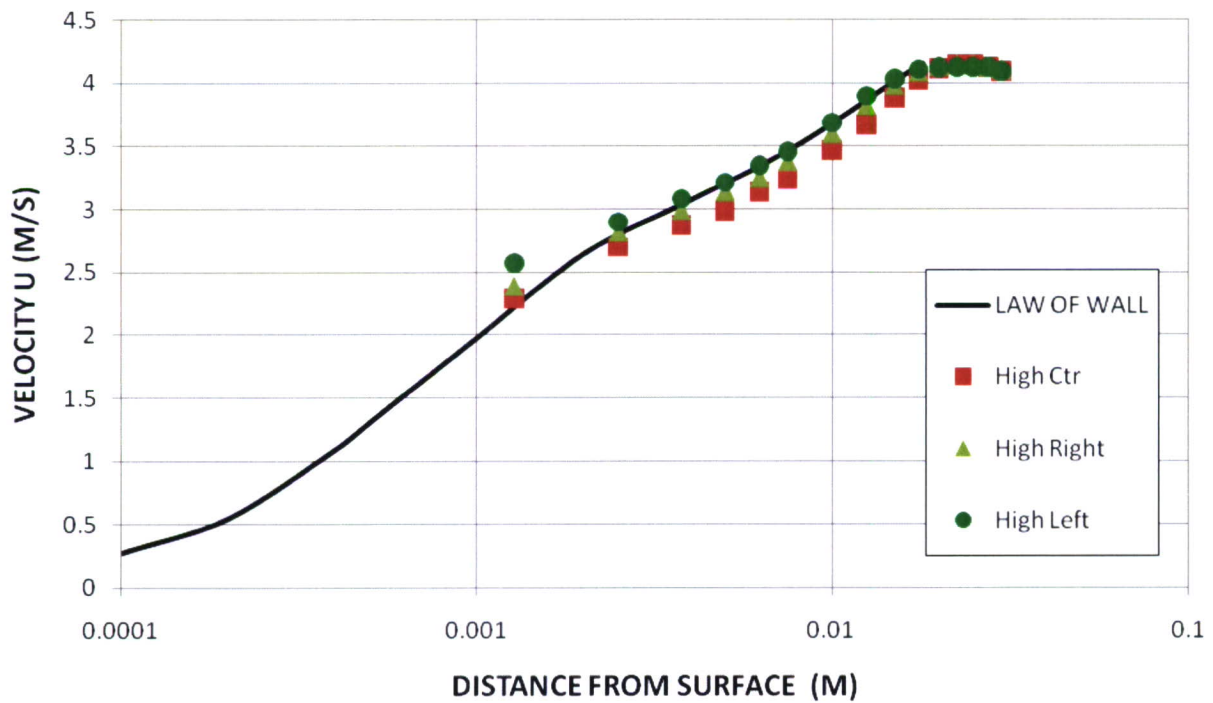


Figure 32. Comparison Between Predicted Law of the Wake Based on Average Parameters and High Wind Speed Data

7. SUGGESTED METHODS OF OPERATION

The following protocol of operation is suggested for using the Conditioning Wind Tunnel when working with multiple samples of persistent agents in conjunction with a 5 cm Agent Fate Wind Tunnel instrumented for vapor measurements.

1. Test environmental conditions (velocity, temperature, and humidity) within the Conditioning Wind Tunnel are set, tunnel started, and sufficient time allowed to stabilize tunnel conditions. Typically, this step will be skipped when the tunnel is already in operation.

2. If a test is in progress, a sample will be removed from the 5 cm Wind Tunnel, placed in a special transport sealed container for safe moving samples between tunnels.

3. Turn off flow in Conditioning Wind Tunnel.

4. Lower the test section floor and slide forward the substrate holder.

5. Select the appropriate sample to be removed and use the extraction piston to assist with the sample's removal. A special transport sealed container will be used to transfer the sample safely to the 5 cm Agent Fate Wind Tunnel for vapor sampling.

6. The removed sample (from Step 5) is loaded into the 5 cm Agent Fate Wind Tunnel for vapor measurements.

7. If a sample was removed from the instrumentation wind tunnel, then place it into the position vacated by Step 5. Adjust the sample height so that it is flush with the top of the sample holder.

8. Slide the test section floor rearward and raise it into the Conditioning Wind Tunnel until it is flush with the fetch and exhaust section floors.

9. After the prescribed measurement time, return to Step 2 for the next sample.

A sequential sampling protocol will automatically provide a simple rotation scheme so that a particular sample is placed into a different position each time it is reintroduced into the Conditioning Wind Tunnel. This will permit each sample to be in each of the eight sample positions, thus being equally affected by upstream samples.

On lowering the test section floor, the samples are also exposed to the atmosphere of the chemical fume hood. This temporally changes the agent volatilization from the sample, as well as the equilibrium condition prevailing in the tunnel test section. Three factors decrease the significance of this operation. First, the airflow in the tunnel is shut off when the test section is opened. Second, the relatively

high wind speed in the tunnel compared to the relatively short time of exposure to the airflow in the hood. Finally, the wind tunnel could be reconfigured to allow vapor measurements of multiple drops.

8. CONCLUSIONS

A Conditioning Wind Tunnel has been designed, built, and characterized for use in efficiently evaluating the long term volatilization of agents in conjunction with a vapor sampling test facility.

The Conditioning Wind Tunnel allows multiple test samples to be conditioned at identical environmental settings that are used in smaller vapor sampling wind tunnels.

Measurement of the interactions among multiple drops can also be performed, which more closely simulates the actual “real world” environment.

The computed friction velocity in the Conditioning Wind Tunnel is 2 % higher than that of the operational profile for 3 and 6 m/s conditions. This compares to the 5 cm Wind Tunnel friction velocity values that were 4 and 7 %, respectively, below that of the two operational values.

The square of the friction velocity is proportional to the velocity slope at the surface. The near surface velocity profile shows good agreement with the operational profile.

The average experimental intercept constant of the log-law (C) at the high wind speed condition is 5% higher than the operational value of 5.0 and for the medium speed case C is 16 % below (omitting the left station as an outlier). The present high and medium results are consistently lower than the 5 cm tunnel data by 20% and 28%, respectively; although, the uncertainty in the calculated 5 cm data is approximately ± 30 %.

The wake profile parameter (D) is somewhat higher than the 5 cm Wind Tunnel; however, the maximum is still significantly less than that of a constant pressure equilibrium boundary layer. The trend of D (also C and the shape factor) with Reynolds confirms the non-equilibrium character of these velocity profiles.

9. RECOMMENDATIONS

A number of modifications to improve the design and operation of the Conditioning Wind Tunnel were realized by working with the first version.

A method for air temperature and humidity control needs to be developed. In conjunction with the supply air conditioning, controlling the temperature of the tunnel

structure is required to reduce possible condensation of chemical vapor on to the internal walls of the tunnel. This could be accomplished by using electrical heat tape, a water jacket, and/or Peltier heating/cooling devices.

Electro-polish and add chemical resistance coating to the Conditioning Wind Tunnel interior surfaces (especially those from the test section through the turning vane section) to reduce the amount of chemicals that would adhere to the inside of the tunnel.

Incorporate a vapor sampling system to allow it to be used to study the interaction of multiple droplets.

Reduce the size of the plenum to allow for more efficient use of fume hood space. Re-characterize the test section velocity profiles to confirm that they still adequately match the operational profiles. This would also involve reducing the inlet holes of the plenum to a 19 mm diameter to better accommodate the supply air system and mass flow controllers.

Add a flange to the entrance to the contraction section and increase the thickness of the downstream side of the plenum to allow a better mechanical connection between the two sections. A gasket could be added to allow an air tight seal.

Add six additional sampling ports in the roof of the test section; three ports forward and three aft of the ceiling windows.

Redesign the test section side windows to allow unobstructed viewing flush with the floor.

Modify the roughening element inserts to fit into recesses in the fetch section floor and ceiling. Machine the roughening section from a solid piece of stainless steel. Blank smooth plates could also be used if no roughening elements were needed.

Redesign the tunnel support system to facilitate height adjustments.

LITERATURE CITED

1. Weber, D.J.; Scudder, M.K.; Moury, C.S.; Shuely, W.J.; Molnar, J.W.; Miller, M.C. *Development of the 5-cm Agent Fate Wind Tunnel*; ECBC-TR-327; U.S. Army Edgewood Chemical Biological Center: Aberdeen Proving Ground, MD, 2006; UNCLASSIFIED Report (AD-A464 938).
2. Weber, D.J.; Scudder, M.K.; Moury, C.S.; Donnelly, T.A.; Park, K.H.; D'Onofrio, T.G.; Molnar, J.W.; Shuely, W.J.; Nickol, R.G; King, B.E.; Danberg, J.E.; Miller, M.C. *Micro Wind Tunnel for Hazardous Chemical Fate Studies*. Presented at the 45th American Institute for Aeronautics and Astronautics (AIAA) Aerospace Sciences Meeting, Reno, Nevada, 8-11 January 2007; AIAA-2007-0960.
3. Waysbort, D.; Manisterski, E.; Leader, H.; Manisterski, B.; Ashani, Y. Laboratory Setup for Long-Term Monitoring of the Volatilization of Hazardous Materials: Preliminary Tests of O-Ethyl S-2-(N,N-Diisopropylamino) ethyl Methylphosphonothiolate on Asphalt. *Environ. Sci. Technol.* **2004**, 38, 2217-2223.
4. Weber, D.J.; Scudder, M.K.; Moury, C.S.; Shuely, W.J.; Molnar, J.W.; Danberg, J.E.; Miller, M.C. *Velocity Profiles Characterization for the 5-cm Agent Fate Wind Tunnels*; ECBC-TR-567; U.S. Army Edgewood Chemical Biological Center: Aberdeen Proving Ground, MD, 2008; UNCLASSIFIED Report (AD-A476 518).
5. Kilpatrick, W.T.; Ling, E.E.; Brevett, C.A.S; Hin, A.R.T. *Experimental Design Requirements for Predictive Model Development Using Agent Fate Wind Tunnels*. AFRL-RH-WP-TR-2008-0102, Air Force Research Laboratory: Wright-Patterson Air Force Base, OH, 2007; UNCLASSIFIED Report (AD-B345 400).
6. Barlowe, J.B.; Rae, W.H.; Pope, A. *Low-Speed Wind Tunnel Testing*; John Wiley & Sons, Inc: New York, 1999, pp 25-102.
7. Bradshaw, P.; Mehta, R. "Wind Tunnel Design", web page <http://navier.stanford.edu/bradshaw/tunnel>, accessed May 2006.
8. D'Onofrio, T. "Quantitative Image Analysis of Agent/Substrate Interactions", In *Proceedings of the 2006 Scientific Conference on Chemical & Biological Defense Research*, Hunt Valley, MD, 13-15 November 2006; SOAR-07-20, [CD-ROM]; Chemical, Biological, Radiological and Nuclear Information Analysis Center: Aberdeen Proving Ground, MD, January 2007.
9. Schlichtning, H.H. *Boundary-Layer Theory*; 7th ed.; McGraw-Hill: New York, 1979.

10. Coles, D.E. The Law of the Wake in the Turbulent Boundary Layer. *J. Fluid Mechanics* **1956**, 1, 191.
11. Tennekes, H.; Lumley, J.L. *A First Course in Turbulence*. The Massachusetts Institute of Technology Press: Cambridge, 1972, p 157.
12. White, Frank M. *Viscous Fluid Flow*. McGraw-Hill: New York, 1974, p 472.
13. Clauser, F.H. *The Turbulent Boundary Layer*, *Advances in Applied Mechanics*; H. L. Dryden & Th. Von Kármán, eds.; Volume IV; Academic Press, Inc.: New York, 1956.
14. Cebeci, T.; Smith, A.M.O. *Analysis of Turbulent Boundary Layers*; Academic Press: New York, 1974, p 125.

APPENDIX

CONDITIONING TUNNEL DESIGN DRAWING

(all dimensions are in centimeters)

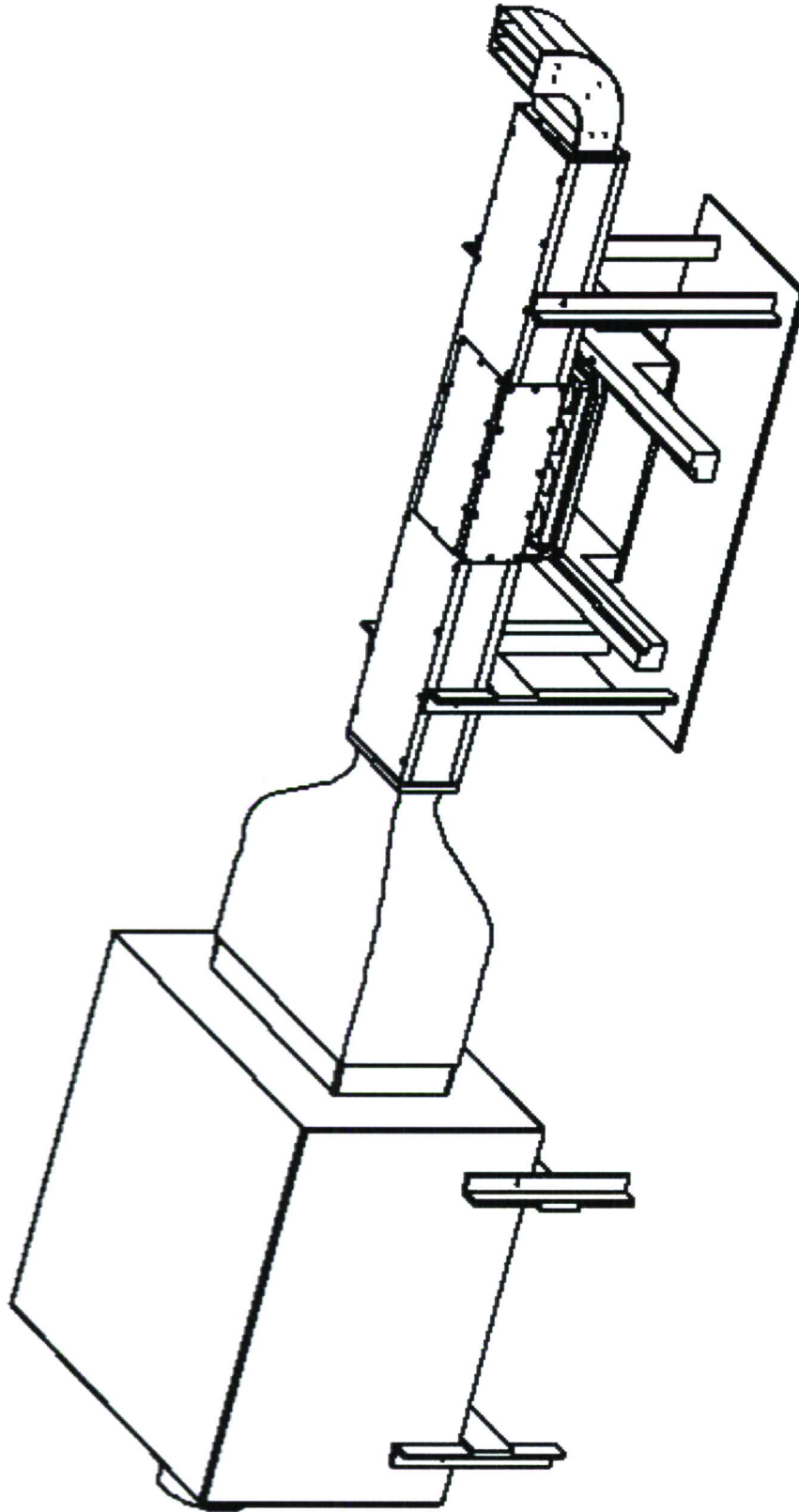


Figure 1. Conditioning Wind Tunnel Isometric View

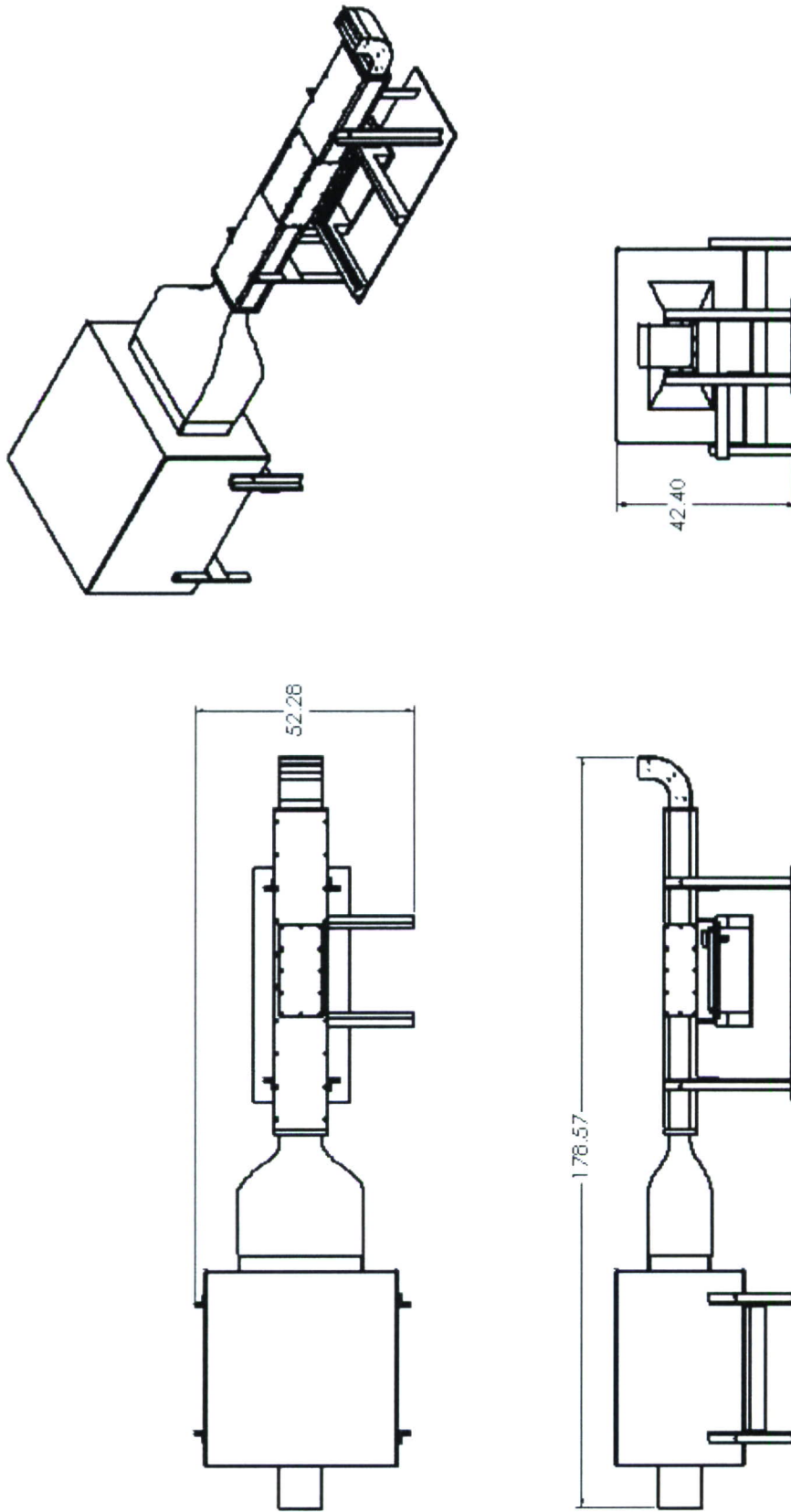


Figure 2. Conditioning Wind Tunnel Overall Dimensions

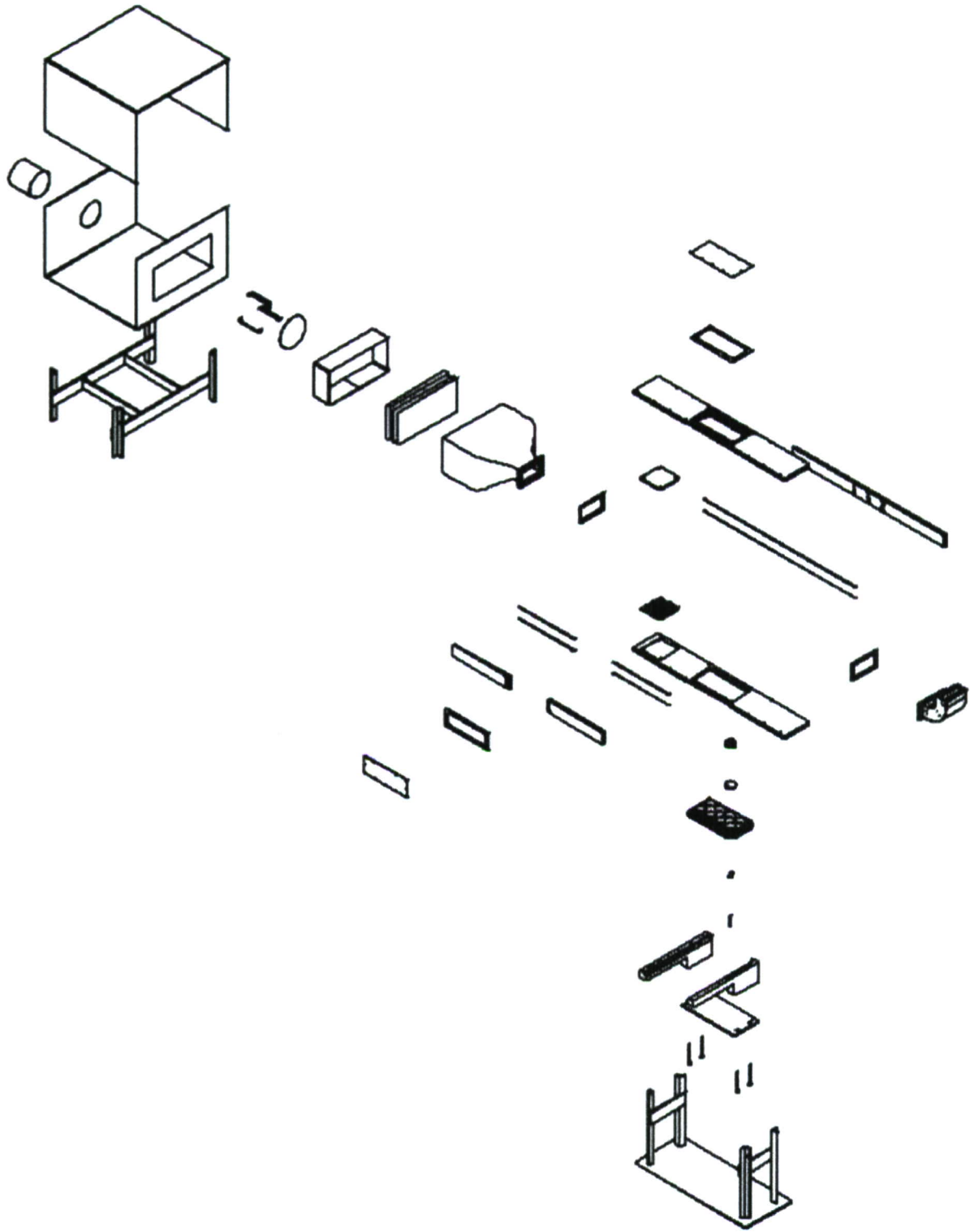


Figure 3. Exploded Parts View of Conditioning Wind Tunnel

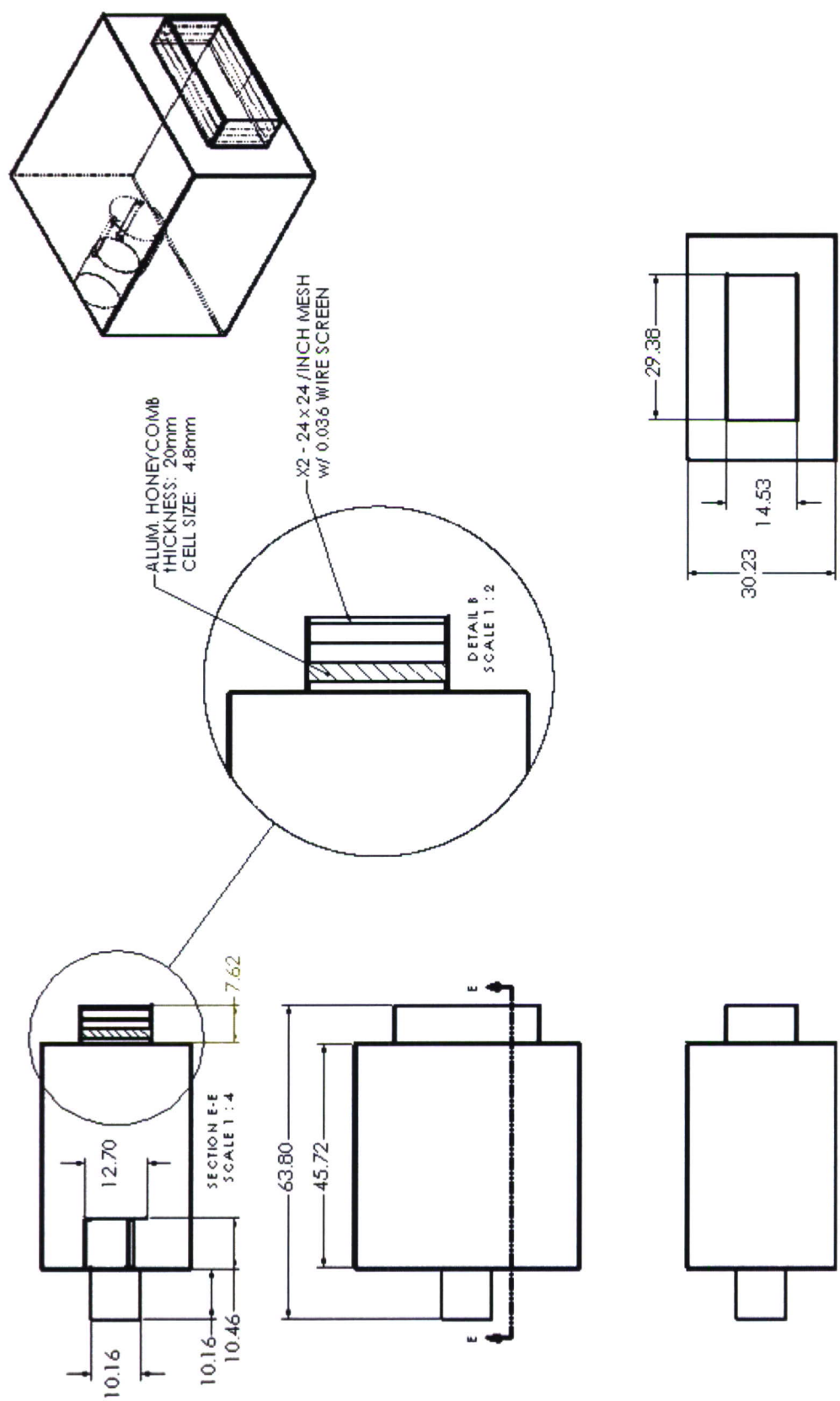


Figure 4. Plenum Box Dimensions and Flow Straighteners

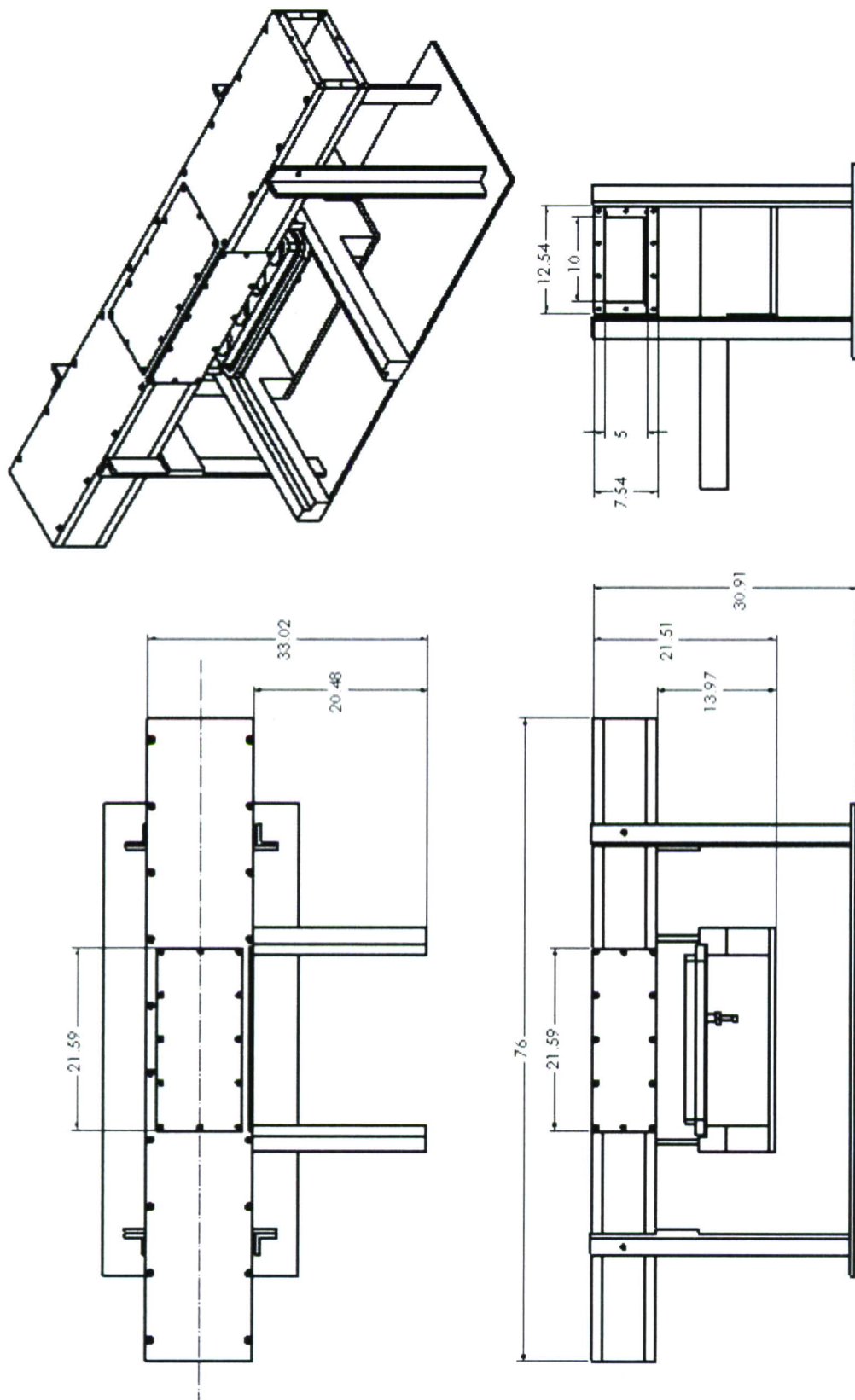


Figure 5. Fetch, Test, and Exit Section Dimensions

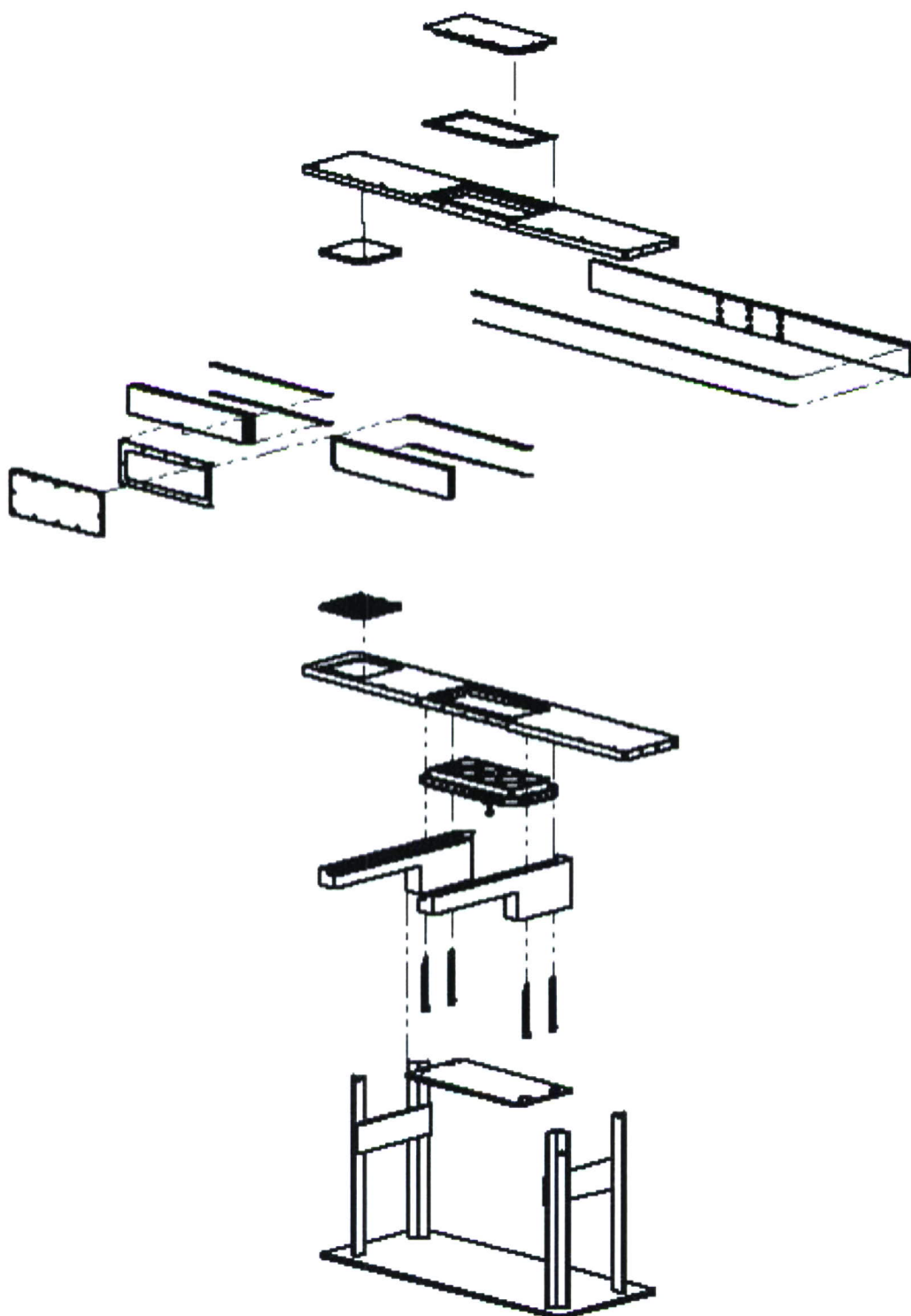


Figure 6. Exploded View of Fetch, Test and Exit Sections

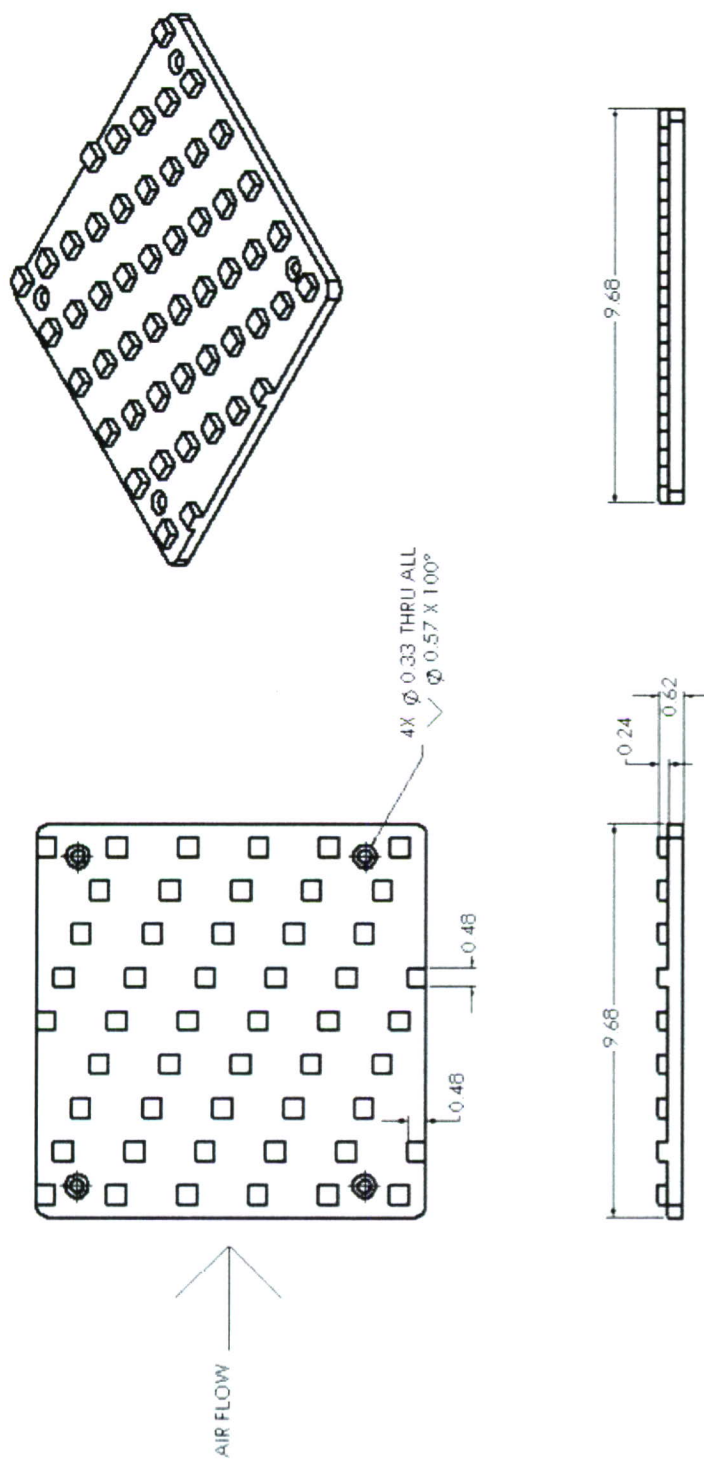


Figure 7. Fetch Section Roughening Elements

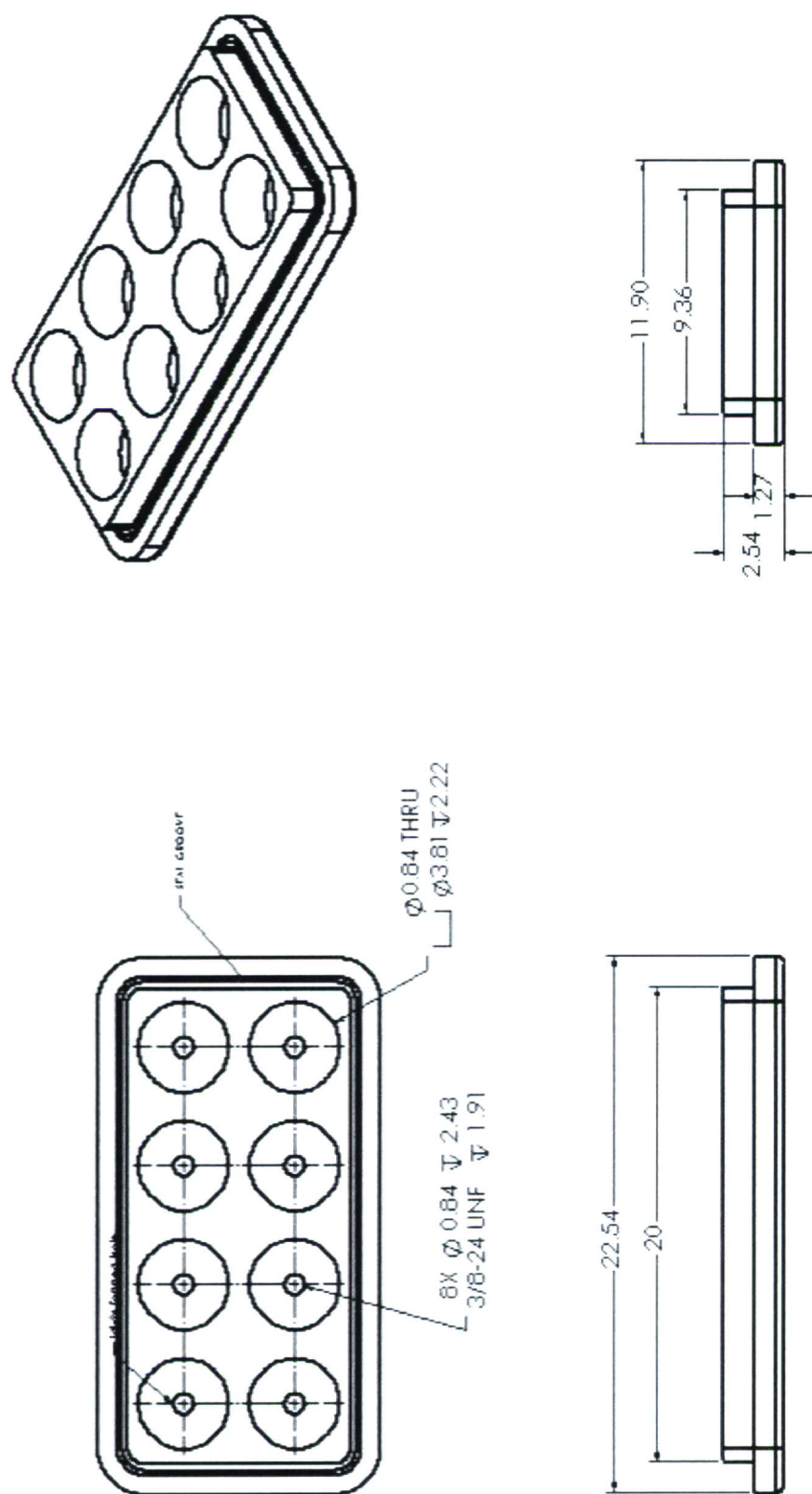


Figure 8. Sample Holder Tray and Test Section Floor Dimensions

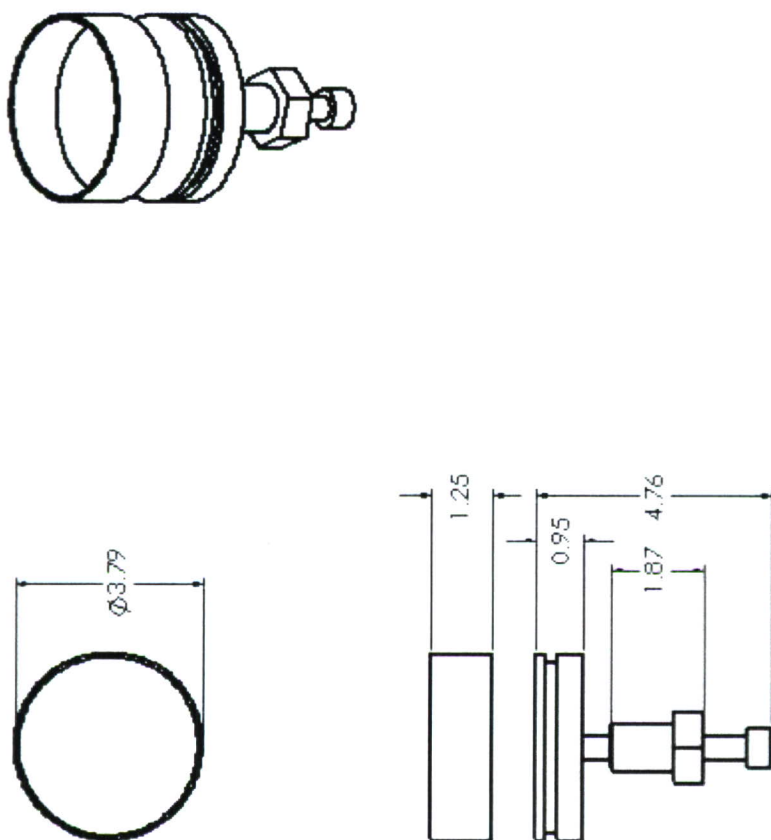
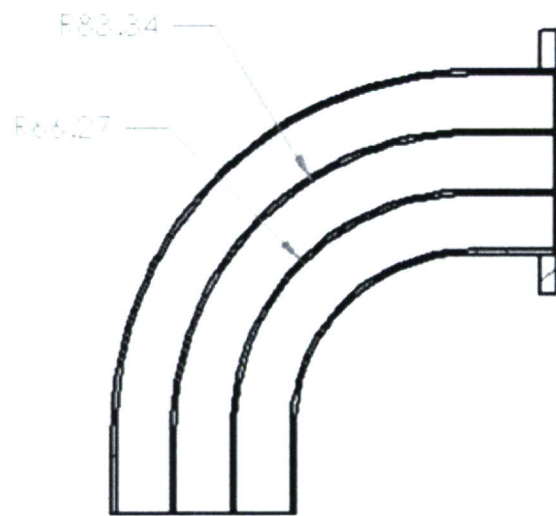
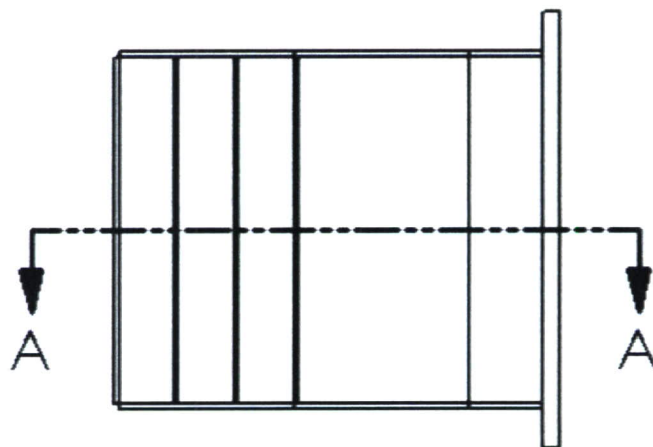


Figure 9. Sample Holder Height Adjuster and Extractor



SECTION A-A
SCALE 1 : 2



TOP VIEW

Figure 10. Exit Turning Vane Section